THE JOURNAL OF BIOLOGICAL CHEMISTRY VOL. 285, NO. 10, pp. 6937–6951, March 5, 2010

p66^{shc} Inhibits Insulin-like Growth Factor-I Signaling via Direct Binding to Src through Its Polyproline and Src Homology 2 Domains, Resulting in Impairment of Src Kinase Activation*[S]

Received for publication, September 24, 2009, and in revised form, December 18, 2009 Published, JBC Papers in Press, January 4, 2010, DOI 10.1074/jbc.M109.069872

Gang Xi, Xinchun Shen, and David R. Clemmons[1]

From the Department of Medicine, University of North Carolina School of Medicine, Chapel Hill, North Carolina 27599

p66^{shc} is increased in response to cell stress, and these increases regulate growth factor actions. These studies were conducted to determine how p66^{shc} alters IGF-I-stimulated Src activation, leading to decreased IGF-I actions. Our results show that p66^{shc} binds to Src through a polyproline sequence motif contained in the CH2 domain, a unique domain in p66^{shc}, and IGF-I stimulates this interaction. Disruption of this interaction using a synthetic peptide containing the p66^{shc} polyproline domain or expression of a p66^{shc} mutant containing substitutions for the proline residues (P47A/P48A/P50A) resulted in enhanced Src kinase activity, p52^{shc} phosphorylation, MAPK activation, and cell proliferation in response to IGF-I. To determine the mechanism of inhibition, the full-length CH2 domain and intact p66^{shc} were tested for their ability to directly inhibit Src kinase activation *in vitro*. The CH2 domain peptide was clearly inhibitory, but full-length p66^{shc} had a greater effect. Deletion of the C-terminal Src homology 2 domain in p66^{shc} reduced its ability to inhibit Src kinase activation. These findings demonstrate that p66^{shc} utilizes a novel mechanism for modulating Src kinase activation and that this interaction is mediated through both its collagen homologous region 2 and Src homology 2 domains.

Shc (Src homology collagen) is an important adaptor protein that couples tyrosine kinase receptor signaling to Ras/MAPK[2] activation. As a result of alternative translation initiation sites and mRNA splicing, a single gene produces three isoforms of Shc, p66/p52/p46^{shc} (1, 2). Three important tyrosines, Tyr^{239}, Tyr^{240}, and Tyr^{317}, in p52^{shc} are phosphorylated following growth factor stimulation. These phosphotyrosines provide binding sites for recruiting Grb2 (growth factor receptor-bound 2), which initiates the sequence of events leading to MAPK activation (3, 4). Therefore, p52^{shc} is believed to play a positive growth-stimulatory role in a variety of cell types (4, 5). More recently, p52^{shc}-mediated signaling has been shown to be essential for tumor progression in mouse models of human breast cancer (6). In smooth muscle cells (SMC), exposed to hyperglycemia, p52^{shc}-mediated signaling has been demonstrated to be important for insulin-like growth factor-I (IGF-I) signaling and biological actions. Following IGF-I receptor stimulation, the integral membrane protein SHPS-1 (Src homology 2 domain-containing protein-tyrosine phosphatase substrate-1) is tyrosine-phosphorylated, and a signaling complex composed of SHP-2 (Src homology 2 domain-containing protein-tyrosine phosphatase-2), c-Src, and p52^{shc} is assembled on SHPS-1. This induction of p52^{shc} phosphorylation and subsequent activation of MAPK enhance the sensitivity of smooth muscle cells to the mitogenic actions of IGF-I (7). This has been demonstrated in cultured cells as well as experimental animals (8). In contrast to p52^{shc}, the p66 isoform of Shc has been shown to inhibit both epidermal growth factor- and IGF-I-stimulated MAPK activation and cell proliferation (2, 9, 10). In addition, p66^{shc} has been shown to regulate the oxidative stress response through its unique CH2 domain (11). p66^{shc} expression is increased during states of oxidative stress (12–14) and hyperglycemia-induced oxidative stress (15, 16). This increase in p66^{shc} is believed to be proapoptotic in some cell types, and genetic ablation of p66^{shc} in mice is associated with reduced generation of ROS in response to hyperglycemia and reduced apoptosis (15, 17, 18).

In SMC, hyperglycemic stress and the increase in reactive oxygen species generation can lead to apoptosis, but if growth factors, including IGF-I, are present, the MAPK and cell proliferation responses are increased (19–22). In this cell type, the phosphorylation of p52^{shc} in response to IGF-I is enhanced by hyperglycemia when compared cells are maintained in 5 mM glucose (23). Importantly, this response of p52^{shc} to IGF-I in response to hyperglycemic stress is modulated by c-Src, which directly phosphorylates p52^{shc} (24). Because both p52 and p66^{shc} isoforms are induced in response to hyperglycemic stress yet they have been reported to mediate different actions, we investigated the role of p66^{shc} in modulating p52^{shc} activation and showed that its overexpression attenuated p52^{shc} phosphorylation and inhibited the mitogenic response to IGF-I (10). Therefore, these studies were undertaken to determine the mechanism by which p66^{shc} modulates IGF-I-stimulated p52^{shc} activation and mitogenesis.

EXPERIMENTAL PROCEDURES

Human IGF-I was a gift from Genentech (South San Francisco, CA). Dulbecco's modified Eagle's medium containing

* This work was supported, in whole or in part, by National Institutes of Health Grants HL56850 and AG02331.

[S] The on-line version of this article (available at http://www.jbc.org) contains supplemental Fig. 1.

[1] To whom correspondence should be addressed: CB 7170, 5030 Burnett-Womack, Division of Endocrinology, University of North Carolina at Chapel Hill, Chapel Hill, NC 27599-7170. Tel.: 919-966-4735; Fax: 919-966-6025; E-mail: david_clemmons@med.unc.edu.

[2] The abbreviations used are: MAPK, mitogen-activated protein kinase; IGF, insulin-like growth factor; SMC, smooth muscle cell(s); pSMC, porcine SMC; SH2 and -3, Src homology 2 and 3, respectively; TNT, transcription/translation; P3A, P47A/P48A/P50A; 3F, Y349F/Y350F/Y427F; WT, wild type; HA, hemagglutinin; NS, not significant.

4500 mg of glucose/liter (DMEM-H), penicillin, streptomycin, and anti-phospho-Y419Src antibody were purchased from Invitrogen. The Grb2 polyclonal antibody and the monoclonal phosphotyrosine antibody (PY99) were purchased from Santa Cruz Biotechnology, Inc. (Santa Cruz, CA). Polyvinyl difluoride membrane (Immobilon P), SHPS-1 antibody, and activated Src were purchased from Millipore Corp. (Billerica, MA). The Src antibody was purchased from EMD Chemicals, Inc. (San Diego, CA). The Shc antibody and the Grb2 monoclonal antibody were purchased from BD Biosciences. The total Erk1/2, phospho-Erk1/2, and HA antibodies were obtained from Cell Signaling (Danvers, MA). Autoradiographic film was purchased from Danville Scientific, Inc. (South Plainfield, NJ). All other reagents were purchased from Sigma unless otherwise stated. Four synthetic peptides were prepared that contained the TAT sequence that confers cell permeability followed by either the proline-rich region of the CH2 domain of p66^{shc} sequence, termed p189 (YARAAARQARALGPILPPLPGD; the underline indicates residues 42–52 in p66^{shc}) or a control peptide that contained an equal number of prolines (YARAARQARAGP-PATPAQPGLH). An additional peptide contained the sequence homologous to Src that contains Tyr^{328}, termed p136 (YARAAARQARAVQLYAVVSEE; the underline indicates residues 325–334 in Src). A tyrosine-phosphorylated form of p136 peptide, termed p226, was used in *in vitro* binding and Src kinase assays as well as in living cells. The peptides were synthesized by the Protein Chemistry Core Facility (University of North Carolina, Chapel Hill, NC). These sequences were verified by mass spectrometry.

Cell Culture—Porcine smooth muscle cells (pSMC) were isolated from porcine aortas using a method that had been previously described (25). The cells were maintained in DMEM-H (25 mM glucose) supplemented with 10% fetal bovine serum (Hyclone, Logan, UT), streptomycin (100 μg/ml), and penicillin (100 units/ml). The cells that were used in these experiments were used between passages 5 and 15. Porcine aortic endothelial cells were isolated from young pigs. The aorta was rinsed through with 37 °C phosphate-buffered solution three times and incubated with medium (M199, Cellgro) containing collagenase (1 mg/ml) for about 5 min. The medium was collected and centrifuged at 3000 rpm for 5 min. The pellet was suspended with the same medium and plated into a 150-cm^2 flask (Corning Glass). After attachment (overnight), the medium was refreshed. The purity of the isolated cells was verified by Von Willebrand factor (Dako) staining and morphological observation. Cells processed in this manner formed a homogenous monolayer. For experiments, the cells were plated in either 10-cm or 6-cm dishes (Corning Glass) and fed with M199 containing 20% fetal bovine serum, 25 mM glucose, streptomycin (100 μg/ml), penicillin (100 unit/ml), and sodium pyruvate (100 nM). The cells that were used in these experiments were used between passages 5 and 10.

Construction of cDNAs and Establishment of p66^{shc} Si, EVC, p66^{shc} WT-HA, p66^{shc} 3F-HA, p66^{shc} P3A-HA, p66^{shc} ΔSH2, Src WT-HA, Src 2F-HA, and LacZ Cells—pSMC expressing small hairpin RNA sequence targeting p66^{shc} (p66^{shc} Si) and corresponding control pSMC expressing empty vector (EVC), pSMC expressing wild type (WT) p66^{shc} (p66^{shc} WT-HA), and corresponding control pSMC expressing LacZ (LacZ) have been described previously (10). In addition, pSMC expressing WT Src (Src WT-HA) and Src Y329F/Y360F (Src 2F-HA) also have been previously described (24). The p66^{shc} WT-HA vector was used as a template to generate the p66^{shc} Y349F/Y350F/Y427F (p66^{shc} 3F) by two rounds of PCR. The first round of PCR generated p66^{shc} Y349F/Y350F using forward and reverse primers: 5′-CCACCTGACCATCAGTTCTTTAATGACTTCCCG-GGG-3′ and 5′-CCCCGGGAAGTCATTAAAGAACTGAT-GGTCAGGTGG-3′. The first round PCR product was used as a template for second round PCR to generate p66^{shc} Y349F/Y350F/Y427F using forward and reverse primers: 5′-TTGA-TGATCCCTCCTTTGTCAACGTCCAGAACC-3′ and 5′-GGTTCTGGACGTTGACAAAGGAGGGATCATCAA-3′. The underlined bases indicate the substitutions that change tyrosine to phenylalanine. The forward and reverse primers that were used to generate the p66^{shc} P47A/P48A/P50A (P3A) mutant were 5′-CATCCCTGGGGGCCATCCTGGCTCCT-CTGGCTGGGGACG-3′ and 5′-CGTCCCCAGCCAGAGG-AGCCAGGATGGCCCCCAGGGATG-3′. The underlined bases indicated the substitutions that change proline to alanine. Point mutations were introduced using standard method (QuikChange, Stratagene (La Jolla, CA)). The p66^{shc} WT-HA vector was used as a template to generate the p66^{shc} SH2 domain deletion mutant (deleting amino acids 487–579, p66^{shc} ΔSH2) by PCR. The forward and reverse primers that were used to generate the PCR product were 5′-cac cat gga tct cct gcc ccc caa g-3′ and 5′-tta AGCGTAATCTGGAACATCGTAT-GGGTA ctc ccc tcg gag ctg ctc agc c-3′. The PCR product contained a Kozak sequence (CACC) at the 5′-end and a HA (capitalized) sequence at the 3′-end. All constructions were verified by DNA sequencing. 293FT cells (Invitrogen) were prepared for generation of virus stocks, and pSMC expressing p66^{shc} 3F-HA and p66^{shc} P3A-HA were established using procedures that were described previously (10).

Immunoprecipitation and Immunoblotting—The cell monolayers were lysed in a modified radioimmunoprecipitation assay buffer (1% Nonidet P-40, 0.25% sodium deoxycholate, 1 mM EGTA, 150 mM NaCl, and 50 mM Tris-HCl, pH 7.5) in the presence of protease inhibitors (10 μg/ml aprotinin, 1 μg/ml leupeptin, 1 mM phenylmethylsulfonyl fluoride, and 1 μg/ml pepstatin) and phosphatase inhibitors (25 mM sodium fluoride and 2 mM sodium orthovanadate). Coimmunoprecipitation was typically performed by incubating 0.5 mg of cell lysate with 1 μg of each of the following antibodies: anti-Shc, Grb2, Src, SHPS-1, or PY99 at 4 °C overnight. The immunoprecipitates were immobilized using protein A or G beads for 2 h at 4 °C and washed three times with the same lysis buffer containing protease and phosphatase inhibitors. The precipitated proteins were eluted in 40 μl of 2× Laemmli sample buffer, boiled for 5 min, and analyzed by SDS-PAGE followed by immunoblotting. Immunoblotting was performed as described previously (10) using a dilution of 1:1000 for anti-Shc, phospho-Erk1/2, Erk1/2, p419Src, and Src and 1:5000 for anti-Grb2. The membranes were striped for repeat immunoblotting only for loading controls. The proteins were visualized using enhanced chemiluminescence (Pierce).

In Vitro Binding Assay—The *in vitro* [^{35}S]methionine (MP Biomedical, Solon, OH)-labeled intact p66^{shc} and p52^{shc}, p66^{shc} P3A mutant, WT CH2 domain, and P3A-mutated CH2 domain of p66^{shc} were generated by a transcription/translation (TNT) reaction (Promega, Madison, WI). An aliquot of the individual TNT mixture (0.4 μM total protein for each) or different combinations of them, as indicated, were incubated with 200 ng of purified active Src (Millipore Corp.) in binding buffer (HEPES, pH 7.6, 50 mM KCl, 1 mM dithiothreitol, 0.5 mM phenylmethylsulfonyl fluoride, 0.2% Triton X-100, and 10% glycerol) in the presence or absence of p189 or p226 (1 μg/ml), using a 100-μl final volume and rotation for 2 h at 4 °C. 0.6 μg of anti-Src antibody and 30 μl (50% slurry) of protein A/G-agarose beads were then added and incubated for another 2 h. After extensive washing with the binding buffer, the precipitated proteins were eluted in 30 μl of 2× Laemmli sample buffer, boiled for 5 min, and separated using 10% SDS-PAGE. The images were developed and analyzed using a Storm860 PhosphorImager (Amersham Biosciences).

In Vitro Src Kinase Assay—Src kinase activity was determined *in vitro* using a Src kinase assay kit (Millipore Corp.). The kinase assay was performed following the manufacturer's instructions. Briefly, the p66^{shc} (WT or P3A mutant), p52^{shc}, and CH2 domain (WT or P3A mutant) were generated by a TNT reaction (Promega). An aliquot of the TNT mixture of each (final concentration 0.4 μM protein) or combinations of them as indicated were incubated with 2.5 units of purified active Src, 150 μM Src kinase substrate peptide (KVEKIGEGTYGVVYK), and 10 μCi of [γ-^{32}P]ATP in Src reaction buffer (25 mM Tris-HCl, pH 7.2, 25 mM $MgCl_2$, 1.25 mM MnCl2, 0.5 mM EGTA, 60 μM sodium orthovanadate, 0.5 mM dithiothreitol, and 100 μm ATP) in the presence or absence of p189 or p226. The mixtures were incubated for 30 min at room temperature. The amount of ^{32}P that was incorporated into the substrate peptide, which reflects the activity of Src kinase, was quantified by a liquid scintillation counter (Packard, Meriden, CT).

Cell Proliferation Assay—Assessment of pSMC proliferation was performed as described previously (26). Briefly, cells were incubated with or without IGF-I (50 ng/ml) in serum-free DMEM-H containing 0.2% platelet-poor plasma for 48 h, and cell number in each well was counted. For assessment of porcine aortic endothelial cell proliferation, cells were plated at 2×10^4 in each well of a 24-well plate in M199 containing 20% fetal bovine serum and 25 mM glucose. The next day, the medium was replaced with M199 containing 0.2% fetal bovine serum and 25 mM glucose. After 14–16 h, the cells were fed with the same medium in the presence or absence of p189 or a control peptide for 2 h of incubation before being exposed or not to IGF-I (50 ng/ml). After incubation for 48 h, the cell number was determined. Each treatment was analyzed in triplicate, and the results represent mean values of three independent experiments.

Cell Migration Assay—Wounding of control and p66^{shc} WT- and p66^{shc} P3A-overexpressing pSMC was performed as described previously (27). The wounded monolayers were exposed to IGF-I (100 ng/ml) for 48 h at 37 °C. The cells were fixed and stained (Diff Quick, Dade Behring, Inc., Newark, DE), and the number of cells migrating into the wound area was counted. At least eight of the previously selected 1-mm areas at the edge of the wound were counted for each data point.

Statistical Analysis—Chemiluminescent images obtained were scanned using a DuoScan T1200 (AGFA, Brussels, Belgium). The band intensities of the scanned images were within the linear range of detection and were analyzed using NIH Image J, version 1.37V. The results that are shown in all experiments are representative of at least three separate experiments unless otherwise stated and expressed as the mean ± S.E. Student's *t* test was used to compare differences between control and treatment groups or control cells and cells expressing mutant proteins. $p \leq 0.05$ was considered statistically significant.

RESULTS

p66^{shc} Inhibits IGF-I Signaling via Disrupting SHPS-1·p52^{shc}·Grb2 Complex Formation—To examine the possibility that p66^{shc} was competitively inhibiting Grb2 binding to p52^{shc}, we substituted the tyrosines in p66^{shc} that have homology to the p52^{shc}-Grb2 binding sites with phenylalanine and expressed this 3F mutant form of p66^{shc} in pSMC. The expression level was comparable with cultures in which WT p66^{shc} had been overexpressed (Fig. 1*A*). p66^{shc} 3F did not associate with Grb2 after IGF-I stimulation (Fig. 1*B*). However, overexpression of p66^{shc} 3F, like p66^{shc} WT, impaired IGF-I-stimulated p52^{shc}-Grb2 recruitment (*e.g.* a 1.20 ± 0.05-fold increase in p66^{shc} 3F cells *versus* a 2.23 ± 0.17-fold increase in LacZ cells after 10-min IGF-I stimulation; $p < 0.05$) (Fig. 1*B*). Similarly, when formation of the SHPS-1 signaling complex was examined following IGF-I stimulation, overexpression of p66^{shc} 3F inhibited IGF-I-dependent p52^{shc} association with SHPS-1 (*e.g.* a 1.46 ± 0.05-fold increase in p66^{shc} 3F *versus* a 2.10 ± 0.04-fold increase in LacZ cells after 10-min IGF-I stimulation; $p < 0.01$) and Grb2 recruitment to the SHPS-1 complex (*e.g.* a 1.35 ± 0.07-fold increase in p66^{shc} 3F *versus* a 2.49 ± 0.11-fold increase in LacZ after 10-min IGF-I stimulation; $p < 0.01$) although it had no effect on IGF-I-stimulated SHPS-1 phosphorylation (Fig. 1*C*). In addition, we detected increased p66^{shc} association with SHPS-1 after IGF-I stimulation in both the p66^{shc} 3F- and WT p66^{shc}-overexpressing cells, compared with LacZ cells, demonstrating that the ability of p66^{shc} to bind to the SHPS-1 complex was not impaired by the 3F mutation (Fig. 1*C*). Because our previous studies have shown that Src kinase phosphorylates p52^{shc} (24) and that p52^{shc} phosphorylation is inhibited constitutively by p66^{shc} overexpression (10), these results suggested that p66^{shc} could be inhibiting Src kinase.

p66^{shc} Binds Directly to Src through Both Polyproline-SH3 and -SH2 Phosphotyrosine Site Interactions—Overexpression of p66^{shc} impaired p52^{shc} recruitment to Src and enhanced p66^{shc} association with Src after IGF-I stimulation (Fig. 2*A*). Similarly, the p66^{shc} 3F mutant bound to Src, and it also impaired p52^{shc}-Src association after IGF-I stimulation (Fig. 2*A*). The amino acid sequences of p66^{shc} and p52^{shc} are identical except for the addition of a unique CH2 domain in the N terminus of p66^{shc}. A PPLP motif is present within the CH2 domain; thus, in addition to the phosphotyrosine-SH2 (Tyr(P)-SH2) domain interaction that occurs between p52^{shc} and Src,

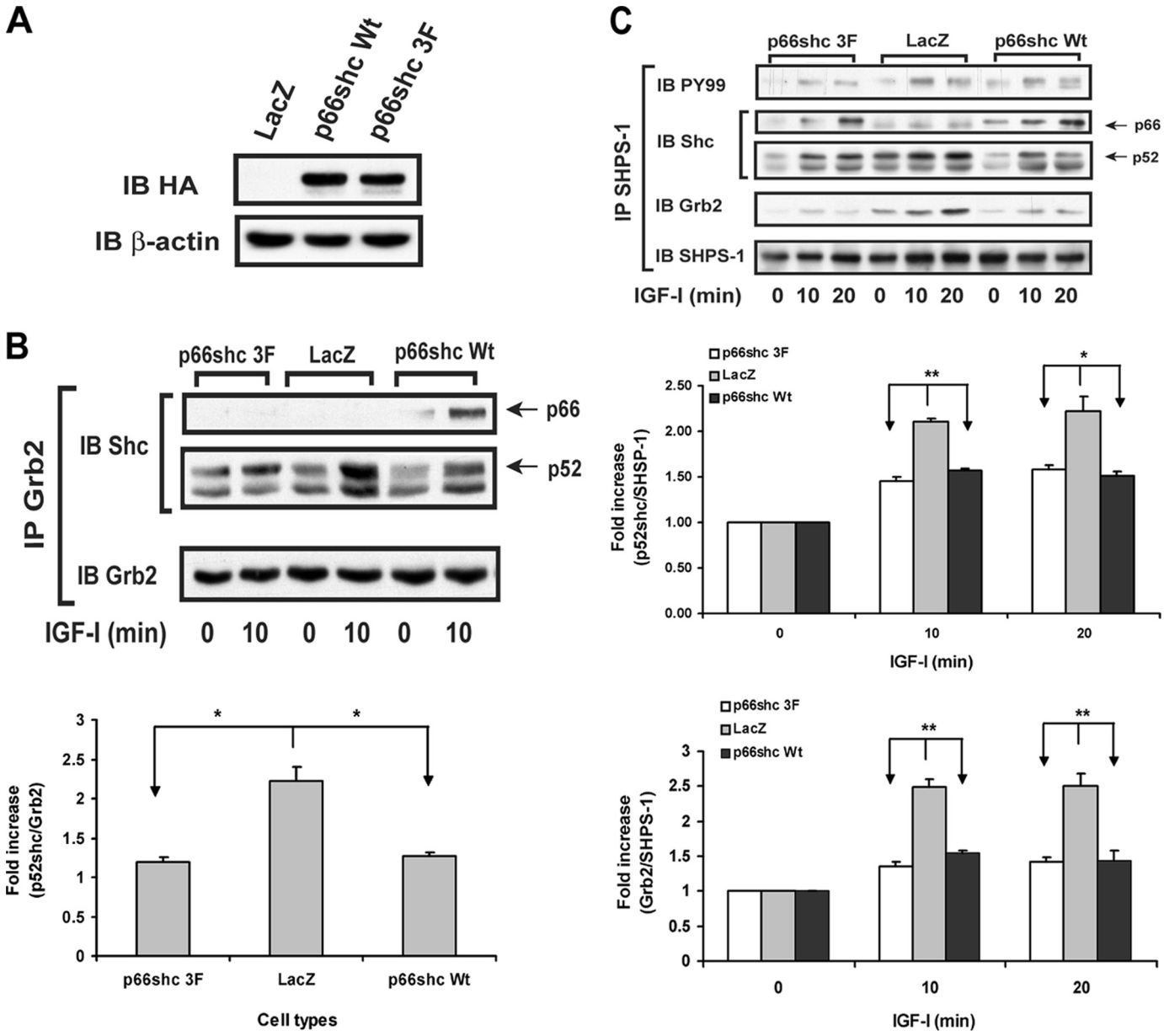

FIGURE 1. **Inhibitory effect of p66^{shc} on IGF-I signaling via disrupting SHPS-1·p52^{shc}·Grb2 complex formation does not require its Grb2 binding ability.** All three cell types were serum-starved for 16–18 h before adding IGF-I (100 ng/ml) for the indicated times. *A*, pSMC were transduced with pLenti-LacZ or pLenti-HA p66^{shc} Y349F/Y350F/Y427F (p66^{shc} 3F) or pLenti-HA p66^{shc} (p66^{shc} WT) vector. Cell lysates were immunoblotted (*IB*) with an anti-HA antibody. *B*, P66^{shc} WT-, LacZ-, and p66^{shc} 3F-overexpressing cell lysates were immunoprecipitated (*IP*) with an anti-Grb2 antibody and immunoblotted with an anti-Shc antibody. To control for loading, the blot was reprobed for an anti-Grb2 antibody. $p < 0.05$ (*) indicates a significant difference between LacZ cells and p66^{shc} WT or p66^{shc} 3F cells at 10 min after IGF-I stimulation. *C*, the cell lysates were immunoprecipitated with an anti-SHPS-1 polyclonal antibody and immunoblotted with anti-Tyr(P) (*PY99*), Shc, or Grb2 antibodies, respectively. To control for loading, the blot was immunoblotted with an anti-SHPS-1 antibody. $p < 0.05$ (*) and $p < 0.01$ (**) indicate significant differences at 10 and 20 min after IGF-I stimulation between LacZ cells and p66^{shc} WT or p66^{shc} 3F cells. The figure is representative of three independent experiments.

p66^{shc} could potentially associate with Src through a P*XX*P-SH3 domain interaction (Fig. 2*B*). To determine if this domain interacted directly with Src, an *in vitro* binding assay was performed using a cell-free expression system. Expression of p66^{shc} and p52^{shc} was detected (Fig. 2*C*, *lanes 1* and *7*). Co-incubation of activated Src with p66^{shc} resulted in their direct association (Fig. 2*C*, *lane 2*). This binding was disrupted by co-incubating with a synthetic peptide, termed p189, which contains the PPLP motif of p66^{shc} (Fig. 2*C*, *lane 3*). As predicted, p52^{shc} bound directly to Src (Fig. 2*C*, *lane 4*). When both p66^{shc} and p52^{shc} were incubated with activated Src, Src binding to p52^{shc} was impaired (Fig. 2*C*, *lane 5 versus lane 4*). This inhibitory effect of p66^{shc} could be reduced by co-incubating with p189 (Fig. 2*C*, *lane 6 versus lane 5*). To further address this question, a p66^{shc} P3A mutant was expressed (Fig. 2*D*, *lane 4*). Compared with WT p66^{shc}, the p66^{shc} P3A mutant had impaired its binding to Src (Fig. 2*D*, compare *lane 1* with *lane 2*). In addition, the binding of WT p66^{shc} to Src could not be disrupted by preincubation with peptide 226, which contains the phosphorylated Y*XX*V (pY*XX*V) motif of Src, the binding site for p52^{shc} (Fig. 2*D*, *lane 2 versus lane 3*). Further supporting data were obtained by expressing the full-length WT CH2 domain (Fig. 2*E*, *lane 1*) and

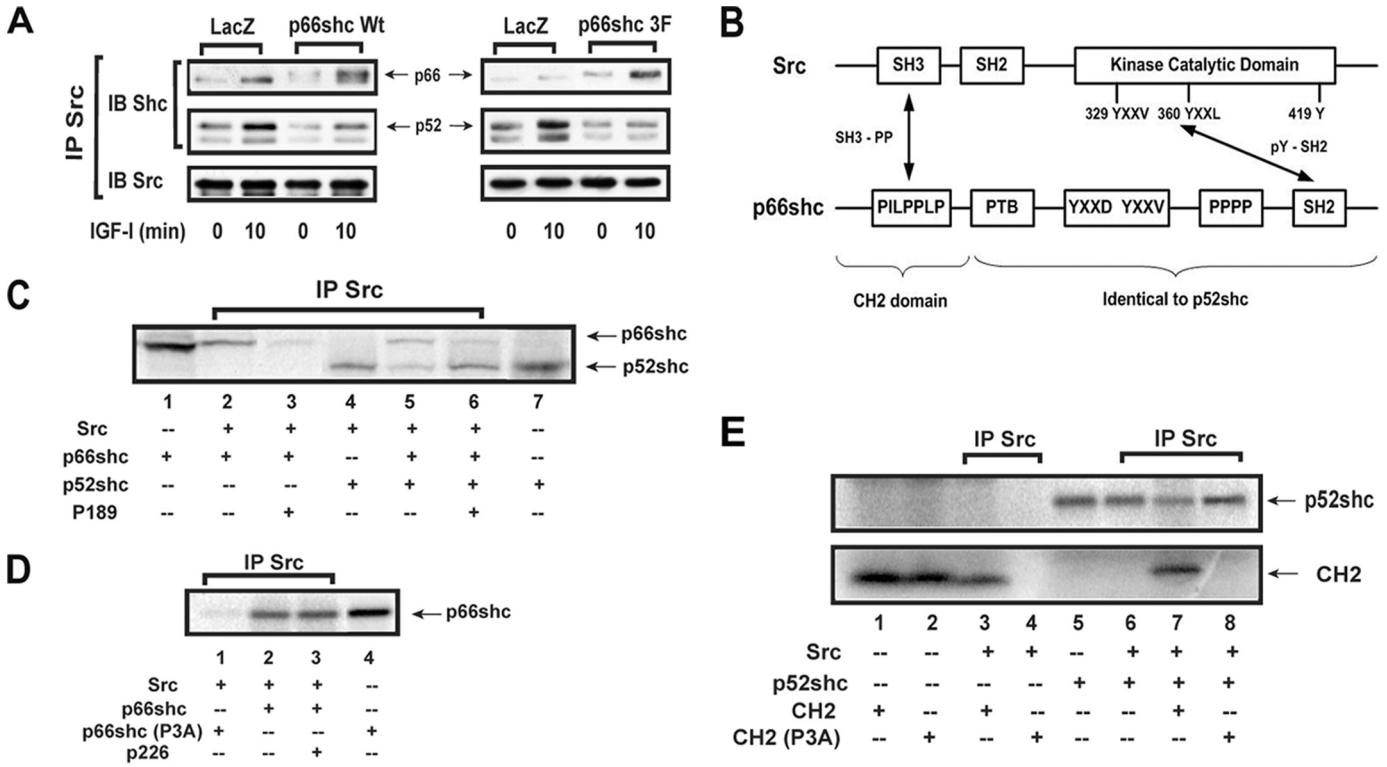

FIGURE 2. **p66^{shc} directly binds to Src through a polyproline-SH3 domain interaction *in vitro*.** *A*, wild type p66^{shc} (p66^{shc} WT)-, LacZ-, and p66^{shc} 3F-overexpressing cells were serum-starved for 16–18 h prior to the addition of IGF-I (100 ng/ml) for the indicated times. The cell lysates were immunoprecipitated (*IP*) with an anti-Src antibody and immunoblotted (*IB*) with an anti-Shc antibody. To control for loading, the blots were stripped and reprobed with an anti-Src antibody. *B*, analysis of potential interactions between Src and p66^{shc}, including SH3 domain-polyproline interaction (*SH3-PP*) and the phosphotyrosine and SH2 domain interaction (*pY-SH2*). *C* and *D*, the ability of p66^{shc}, p52^{shc}, or the p66^{shc} P3A mutant to bind to Src and of the synthetic peptide p189 or p226 to disrupt Src interaction with p66^{shc} and p52^{shc} was determined using *in vitro* binding assays as described under "Experimental Procedures." *E*, the interaction of intact CH2 domain or P3A-mutated CH2 domain and/or p52^{shc} with Src was determined as described for *C* and *D*. ^{35}S-Labeled p66^{shc}, p52^{shc}, p66^{shc} (P3A), CH2, and CH2 (P3A) were visualized by using a PhosphorImager. The figure is representative of at least two independent experiments.

P3A mutant CH2 domain (Fig. 2*E*, *lane 2*) and testing their ability to bind to Src. The results showed that the WT CH2 domain, but not P3A mutant CH2 domain, could directly bind to Src (Fig. 2*E*, *lane 3 versus lane 4*). Co-incubation of the CH2 domain peptide with p52^{shc} and Src resulted in a 69 ± 6% decrease in p52^{shc}-Src association (Fig. 2*E*, *lane 6 versus lane 7*), but the P3A mutant CH2 domain had no effect (Fig. 2*E*, *lane 8*). These *in vitro* binding assay results indicate that p66^{shc} can directly bind to Src through a P*XX*P-SH3 domain interaction, and this impairs p52^{shc}-Src association.

Because this interaction has the potential to lead to a conformational change in Src that could impair either Src activation or its ability to bind to p52^{shc}, we investigated the effect of the Src-p66^{shc} interaction on these signaling events. In p66^{shc}-overexpressing cells, p66^{shc} (HA) binding to Src occurred after 1 min of IGF-I treatment and did not further increase after 3 min (Fig. 3*A*, 2.6-fold *versus* 3.0-fold). In LacZ cells, p66^{shc} binding to Src was increased after 1-min IGF-I treatment and further enhanced after 3 min of IGF-I stimulation (Fig. 3*A*, 2.6-fold *versus* 5.6-fold). However, the fold increase in LacZ- and p66^{shc}-overexpressing cells cannot be compared because, in order to clearly show the increase in Src-associated p66^{shc} in LacZ cells, more cell lysate had to be used for co-immunoprecipitation. The Src-p66^{shc} interaction at 1 min could be significantly disrupted by incubating with p189 (4.6-fold *versus* 2.8-fold), whereas the 3-min interaction could only be partially disrupted (Fig. 3*B*, 9.1-fold *versus* 5.2-fold). In contrast, p136, a peptide containing the Y*XX*V motif of Src that binds to the SH2 domain in p52^{shc}, only reduces this interaction after 3-min of IGF-I stimulation (Fig. 3*B*, 9.1-fold *versus* 4.8-fold) but not after 1 min of IGF-I stimulation. Incubating with both p189 and p136 had an even greater effect after 3-min IGF-I stimulation (Fig. 3*B*, 9.1-fold *versus* 2.2-fold). To confirm that the response to p136 was due to the phosphorylated tyrosine, we examined these interactions using a tyrosine-phosphorylated peptide, p226, and nontransduced pSMC. Similar results were obtained (Fig. 3*C*). Of note, there was a slight variation in the effect of p136 or p226 on p66^{shc}·Src complex formation at 1 min of IGF-I treatment (Fig. 3, *B* and *C*, *lane 4 versus lane 2*). However, after standardization using total Src protein and pooling the results from three independent experiments, no significant difference was detected between IGF-I alone and IGF-I plus p136 or p226. These data suggest that the binding of p66^{shc} to Src is initially mediated through P*XX*P-SH3 domain interaction after 1 min of IGF-I stimulation and through both P*XX*P-SH3 and SH2-Tyr(P) interactions after 3 min of IGF-I stimulation in living cells.

To further address this question, we utilized mutagenesis of full-length p66^{shc} to disrupt the P*XX*P-SH3 domain interaction. Three prolines in the CH2 domain of p66^{shc} were substituted with alanines. Expression of this mutant p66^{shc} (p66^{shc} P3A) was verified by HA expression, and the expression level was

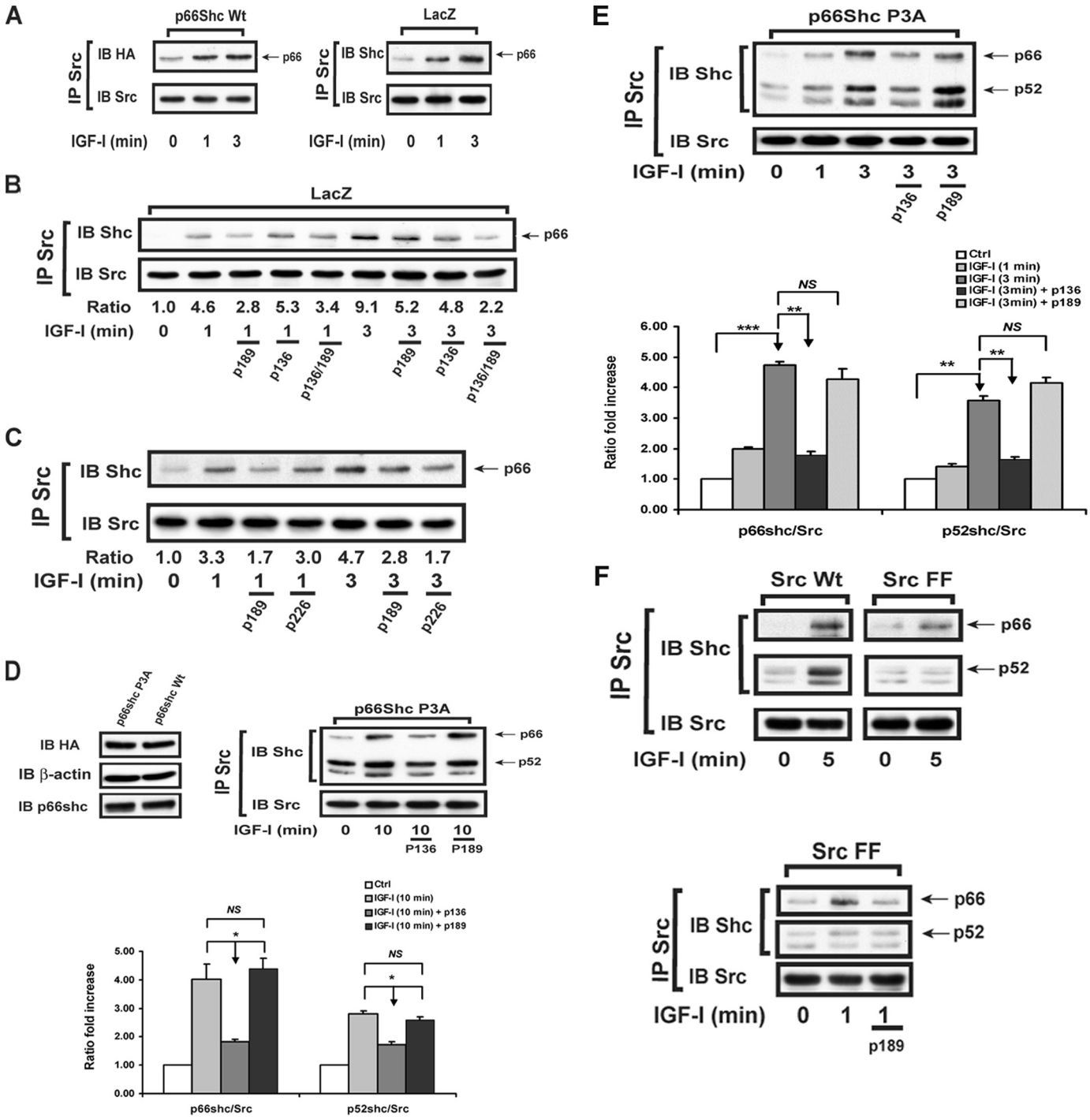

FIGURE 3. **p66^{shc} binds to Src through both polyproline-SH3 and SH2-phosphotyrosine interactions in living cells.** *A*, pSMC were transduced with pLenti-LacZ (*LacZ*) or pLenti-HA p66^{shc} (*p66^{shc} WT*) vector. Both cell types were serum-starved for 16–18 h before stimulation with IGF-I (100 ng/ml) for the indicated times. Cell lysates (p66^{shc} WT, 500 μg of protein; LacZ, 750 μg of protein) were immunoprecipitated (*IP*) with an anti-Src antibody and immunoblotted (*IB*) with an anti-Shc antibody. To control for loading, the blots were reprobed with anti-Src antibody. The *arrow* denotes the p66^{shc} band. *B* and *C*, quiescent LacZ cells (*B*) or non-transduced wild type pSMC (*C*) were preincubated with p189 and/or p136 or p226 (5 μM) as indicated for 2 h and treated with IGF-I (100 ng/ml) for the indicated times. The cell lysates were immunoprecipitated with an anti-Src antibody and immunoblotted with an anti-Shc antibody. To control the loading, the blot was reprobed with an anti-Src antibody. The *arrow* denotes the p66^{shc} band. The ratio represents the densitometry value of Src-associated p66^{shc} divided by the densitometry value of total Src in each individual *lane*. *D* and *E*, cell lysates from quiescent wild type p66^{shc} (*p66^{shc} WT*)- and P47A/P48A/P50A mutated p66^{shc} (*p66^{shc} P3A*)-overexpressing cells were analyzed for HA protein expression by immunoblotting with an anti-HA antibody. Quiescent p66^{shc} P3A-overexpressing cells were incubated with or without p189 or p136 (5 μM) as indicated for 2 h before being exposed to IGF-I (100 ng/ml) for the indicated times. The cell lysates were immunoprecipitated with an anti-Src antibody and immunoblotted with an anti-Shc antibody. The *arrows* denote the p66^{shc} and p52^{shc} bands. $p < 0.05$ (*) indicates that p136 preincubation significantly impairs p66^{shc} and p52^{shc} binding to Src after IGF-I stimulation, compared with without a peptide or p189 preincubation in p66^{shc} P3A cells (for *D*). $p < 0.01$ (**) and $p < 0.001$ (***) indicate that 3 min of IGF-I stimulation significantly enhances p66^{shc} and p52^{shc} association with Src in p66^{shc} P3A (for *E*). *F*, pSMC were transduced with pLenti-wild type Src (*Src WT*) or pLenti-Y329F/Y360F Src (*Src FF*) vectors. Quiescent cells were incubated with or without p189 for 2 h and then stimulated with IGF-I (100 ng/ml) for the indicated times. Cell lysates were immunoprecipitated with an anti-Src antibody, followed by immunoblotting with an anti-Shc antibody. To control for loading, the blot was reprobed with an anti-Src antibody. The *arrows* denote the p66^{shc} and p52^{shc} bands. The figure is representative of three independent experiments.

comparable with WT p66^{shc} (p66^{shc} WT) (Fig. 3*D*). Overexpression of p66^{shc} P3A did not impair IGF-I-stimulated p66^{shc} binding to Src, which was clearly increased after 10 min (*e.g.* 4.03 ± 0.52-fold increase above basal level after 10-min IGF-I stimulation; $p < 0.05$). In contrast to cells overexpressing WT p66^{shc}, Src-p52^{shc} association was increased to a greater extent (*e.g.* a 2.82 ± 0.10-fold increase in p66^{shc} P3A cells *versus* a 1.53 ± 0.09-fold increase in p66^{shc} WT cells after 10-min IGF-I stimulation; $p < 0.01$) (Fig. 3*D versus* Fig. 2*A*). This association was not significantly affected by preincubating with p189, which disrupts the P*XX*P-SH3 domain interaction. However, preincubating with peptide p136, which blocks the SH2-Tyr(P) interaction, inhibited both p66^{shc}-Src (*e.g.* a 4.03 ± 0.52-fold increase with no peptide preincubation *versus* a 1.82 ± 0.08-fold increase with p136 preincubation after 10-min IGF-I stimulation; $p < 0.05$) and p52^{shc}-Src interactions (*e.g.* a 2.82 ± 0.10-fold increase with no peptide preincubation *versus* a 1.72 ± 0.10-fold increase with p136 preincubation after 10-min IGF-I stimulation; $p < 0.05$) (Fig. 3*D*). This suggested that p66^{shc} bound to Src via a SH2-Tyr(P) domain interaction in p66^{shc} P3A-overexpressing cells. Because analysis of the time course of binding to each of the two sites indicated that the P*XX*P/SH3 interaction occurred at 1 min after IGF-I stimulation, a detailed time course analysis of this interaction using cells expressing the mutant was undertaken. The results indicated that a significant increase in IGF-I-dependent p66^{shc} binding to Src did not occur until 3 min of IGF-I treatment in cells expressing p66^{shc} P3A (*e.g.* a 4.73 ± 0.12-fold increase above basal level after 3-min IGF-I treatment; $p < 0.001$) (Fig. 3*E*). Similarly, a major increase in p52^{shc} binding to Src could be detected after 3 min of exposure to IGF-I (*e.g.* a 3.56 ± 0.16-fold increase above basal level after 3-min IGF-I stimulation; $p < 0.01$) (Fig. 3*E*). We conclude that this interaction is mediated via the SH2-Tyr(P) domain interaction, which can be disrupted by p136 incubation (*e.g.* a 3.56 ± 0.16-fold increase with no peptide preincubation *versus* a 1.66 ± 0.07-fold increase in p136 preincubation after 3-min IGF-I treatment; $p < 0.01$) but not p189 (*e.g.* a 3.56 ± 0.16-fold increase with no peptide preincubation *versus* a 4.16 ± 0.17-fold increase with p189 preincubation after 3-min IGF-I treatment; *p*, not significant (NS)) (Fig. 3*E*). To further determine the importance of the Y*XX*(V/L)-SH2 domain interaction for p66^{shc} binding, the two tyrosines in Src that mediate the p52^{shc}-Src interaction were substituted with phenylalanines (Src FF mutant). Overexpression of the Src FF mutant in pSMC significantly impaired both IGF-I-stimulated p52^{shc} and p66^{shc} recruitment to Src, compared with overexpression of Src WT after 5-min treatment (Fig. 3*F*). This confirms that, like p52^{shc}, p66^{shc} also binds to Src through SH2-Tyr(P) interaction after IGF-I stimulation. However, upon IGF-I stimulation, an increase of p66^{shc} bound to Src was still detected in Src FF cells at the 1-min time point. That this is mediated via the P*XX*P-SH3 interaction was confirmed by showing that its binding could be disrupted by p189 preincubation. In contrast, there was no change of p52^{shc}-Src interaction after IGF-I stimulation in Src FF cells at the same time (Fig. 3*F*).

The Inhibitory Effect of p66^{shc} on IGF-I-stimulated Downstream Signaling and Biological Actions Requires Its Binding to Src via PXXP-SH3 Domain Interaction—Overexpression of p66^{shc} impaired IGF-I-stimulated p52^{shc} phosphorylation compared with cells expressing LacZ (*e.g.* a 1.84 ± 0.07-fold increase in LacZ cells *versus* a 1.15 ± 0.10-fold increase in p66^{shc} WT cells after 10-min IGF-I stimulation; $p < 0.01$) (Fig. 4*A*). This inhibition could be reduced by preincubation with p189 (*e.g.* a 1.69 ± 0.04-fold increase following p189 preincubation *versus* a 1.15 ± 0.10-fold increase with no peptide preincubation after 10-min IGF-I stimulation; $p < 0.01$) but not by a control peptide (Fig. 4*A*). Similarly, overexpression of the p66^{shc} P3A mutant, which was comparable with WT p66^{shc} overexpression, had no inhibitory effect on IGF-I-stimulated p52^{shc} phosphorylation (*e.g.* a 2.39 ± 0.09-fold increase in LacZ cells *versus* a 2.19 ± 0.05-fold increase in p66^{shc} P3A cells after 10-min IGF-I stimulation; *p*, NS) (Fig. 4*B*). When downstream signaling changes were analyzed using WT p66^{shc}-overexpressing cells, incubation with p189 significantly increased IGF-I-stimulated MAPK activation, compared with no peptide or preincubation with a control peptide (*e.g.* a 7.88 ± 0.23 fold *versus* a 2.85 ± 0.20-fold or 3.20 ± 0.21-fold increase after 10-min IGF-I stimulation; $p < 0.01$) (Fig. 4*C*). Consistently, overexpression of p66^{shc} P3A, unlike the WT p66^{shc}, had no inhibitory effect on IGF-I-stimulated Erk1/2 phosphorylation (*e.g.* a 4.25 ± 0.24-fold increase in p66^{shc} P3A cells *versus* a 4.85 ± 0.32-fold increase in LacZ cells after 10 min of IGF-I stimulation; $p < 0.01$) (Fig. 4*D*).

Because disruption of p66^{shc} binding to Src through P*XX*P-SH3 domain interaction significantly attenuated the inhibitory effect of p66^{shc} on IGF-I signal transduction, we determined whether this change could lead to alterations of IGF-I-stimulated biological actions. Overexpression of WT p66^{shc} significantly impaired IGF-I-stimulated cell proliferation, compared with LacZ cells (1.35 ± 0.05-fold *versus* 2.02 ± 0.08-fold increase ($p < 0.01$), a 66% reduction compared with the maximal response) (Fig. 5*A*). However, overexpression of p66^{shc} P3A had no inhibitory effect on the IGF-I-stimulated cell proliferation, compared with LacZ cells (1.90 ± 0.04-fold *versus* 2.02 ± 0.08-fold increase; *p*, NS) (Fig. 5*A*). Of note, for primary pSMC, the maximum response to 10% fetal calf serum is only a 3-fold increase in cell number in 48 h. Similarly, overexpression of p66^{shc} significantly attenuated the ability of IGF-I to stimulate cell migration (1.53 ± 0.09-fold *versus* 2.07 ± 0.08-fold increase, compared with LacZ cells ($p < 0.01$), a 50% reduction compared with the maximal response) (Fig. 5*B*). In contrast, overexpression of p66^{shc} P3A did not inhibit the ability of IGF-I to stimulate cell migration, compared with LacZ cells (1.90 ± 0.03-fold *versus* 2.07 ± 0.08-fold increase after IGF-I stimulation; *p*, NS) (Fig. 5*B*).

Determination of the Mechanism by Which p66^{shc} Inhibits Src Activation—We have previously shown that Src activation (phosphorylation of Tyr^{419}, equivalent to Tyr^{416} in chicken Src), followed by phosphorylation of Tyr^{329} and Tyr^{360}, is required for Src-p52^{shc} association (24). Because p66^{shc} can bind directly to Src after IGF-I stimulation independently of Tyr^{329} and Tyr^{360} phosphorylation and this inhibits p52^{shc} phosphorylation, we determined if the binding of p66^{shc} to Src could alter IGF-I-stimulated Src activation. Cells expressing p66^{shc} short hairpin RNA showed a 87 ± 2% decrease in p66^{shc}

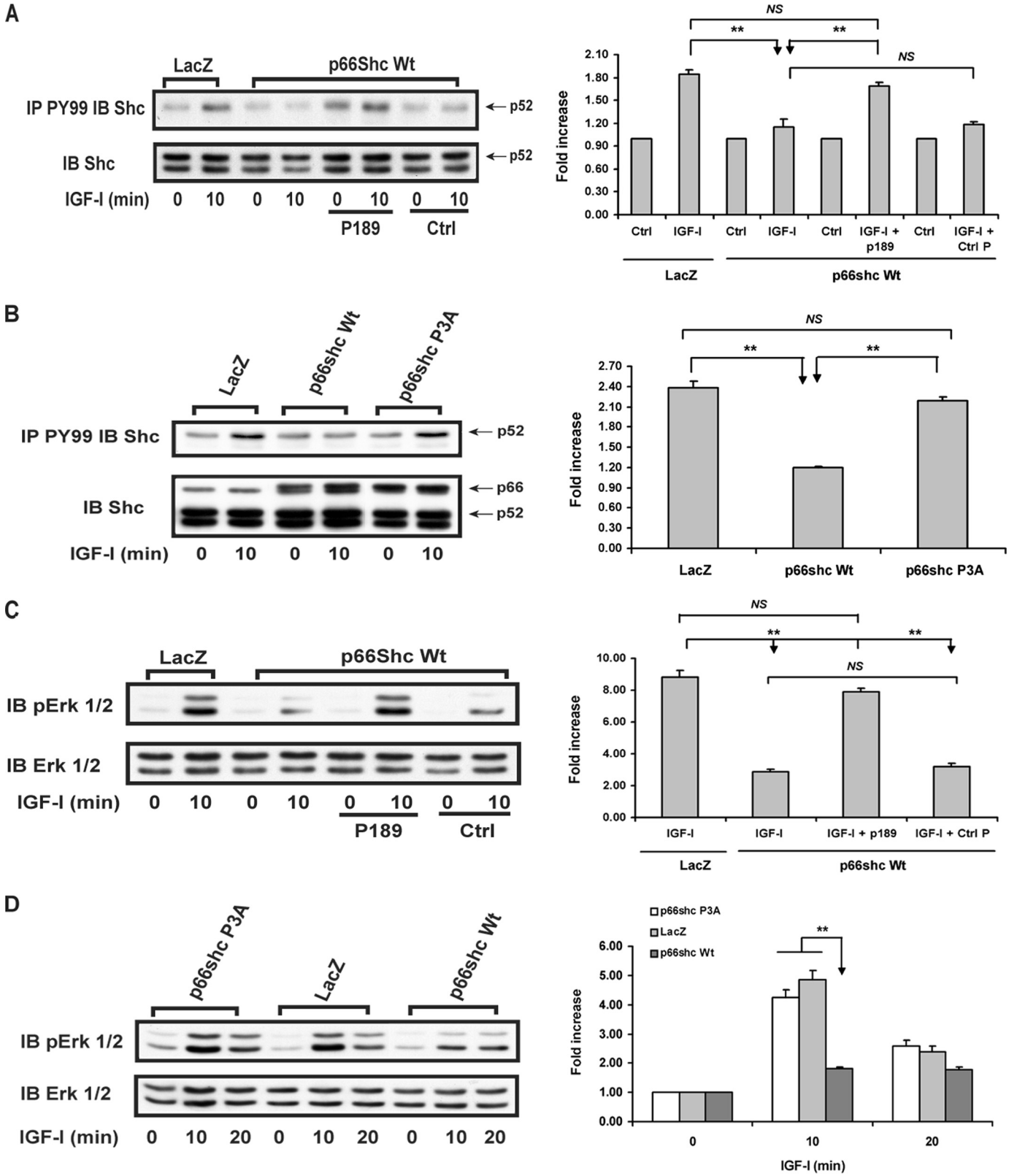

FIGURE 4. **Inhibitory effect of p66^{shc} on IGF-I-stimulated p52^{shc} tyrosine phosphorylation and MAPK activation is dependent on its binding to Src through the polyproline-SH3 domain interaction.** Quiescent LacZ-, wild type p66^{shc} (*p66^{shc} WT*)-, and p66^{shc} P3A mutant-overexpressing cells were incubated with or without the synthetic peptide 189 or control peptide for 2 h before adding IGF-I (100 ng/ml) for the indicated times. *A* and *B*, cell lysates were immunoprecipitated (*IP*) with an anti-Tyr(P) (*PY99*) antibody and immunoblotted (*IB*) with an anti-Shc antibody. To control for loading, an equal amount of cell lysate was immunoblotted with an anti-Shc antibody. $p < 0.01$ (**) indicates a significant difference between two different treatments or the same treatment in two cell types. The *arrows* denote the p52^{shc} and p66^{shc} bands. *C* and *D*, the same cell lysates were used to determine the Erk1/2 phosphorylation by probing with an anti-phospho-Erk1/2 antibody. The blots were reprobed with an anti-Erk1/2 antibody to control for loading differences. $p < 0.01$ (**) indicates a significant difference between two different treatments or the same treatment in two cell types. The figure is representative of three independent experiments.

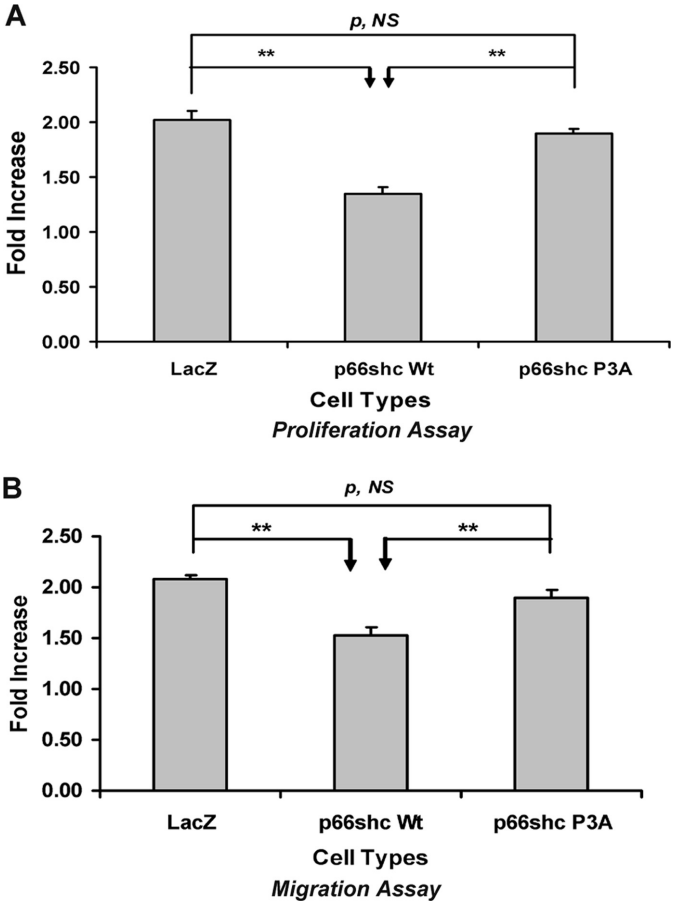

FIGURE 5. **Inhibitory effect of p66^{shc} on IGF-I-stimulated proliferation and migration is dependent on its binding to Src through polyproline-SH3 interaction.** Cell proliferation and migration were determined as described under "Experimental Procedures." *A*, comparison of the cell-proliferative response to IGF-I (50 ng/ml) among wild type p66^{shc} (*p66^{shc} WT*)-, p66^{shc} P3A-, and LacZ-overexpressing cells, respectively. Each *bar* indicates the fold increase over basal level and represents the pool of at least three independent experiments. Cells overexpressing wild type p66^{shc} showed a significant impairment of IGF-I-stimulated cell proliferation, compared with control LacZ- and p66^{shc} P3A-overexpressing cells, respectively. *B*, comparison of cell migration response to IGF-I (100 ng/ml) among p66^{shc} WT-, p66^{shc} P3A-, and LacZ-overexpressing cells, respectively. Each *bar* indicates the fold increase over basal and represents the pool of at least three independent experiments. Overexpression of wild type p66^{shc} significantly attenuated IGF-I-stimulated cell migration, compared with LacZ- and p66^{shc} P3A-overexpressing cells, respectively.

(Fig. 6*A*) compared with empty vector control. IGF-I stimulated Src tyrosine 419 phosphorylation (an index of Src activation) after a 1-min treatment, and this response was enhanced by p66^{shc} knockdown (*e.g.* a 1.81 ± 0.07-fold increase in EVC *versus* a 2.53 ± 0.08-fold increase in p66^{shc} Si; $p < 0.001$) (Fig. 6*A*). This suggests that constitutive expression of p66^{shc} inhibits IGF-I-dependent Src activation. To determine if p66^{shc} inhibits Src activation directly, we performed an *in vitro* Src kinase assay. The results showed that p66^{shc} directly inhibited Src activation in a dose-dependent manner (Fig. 6, *B* and *C*, *lane 2 versus lane 1*; $p < 0.001$). Because we had shown (Fig. 2) that p66^{shc} interacted with Src through its P*XX*P sequence, we determined if the short peptide containing this sequence p189 could inhibit Src activation. The peptide alone had no effect (Fig. 6*C*, *lane 7 versus lane 1*; *p*, NS). However, p189 completely blocked the inhibitory effect of p66^{shc} on Src activation (Fig. 6*C*, *lane 5 versus lane 1*; *p*, NS). Although p226, the peptide that blocked the SH2-Tyr(P) interaction, was unable to completely abolish the inhibitory effect of WT p66^{shc} on Src activity (Fig. 6*C*, *lane 6 versus lane 1*; $p < 0.001$), it partially rescued Src kinase activity in the presence of WT p66^{shc} (Fig. 6*C*, *lane 6 versus lane 2*; $p < 0.01$). However, it was much less effective than p189 (Fig. 6*C*, *lane 6 versus lane 5*; $p < 0.001$). Interestingly, the CH2 domain alone also impaired Src kinase activity (Fig. 6*C*, *lane 4 versus lane 1*; $p < 0.01$), but its effect was less than that of full-length WT p66^{shc} (Fig. 6*C*, *lane 4 versus lane 2*; $p < 0.001$). Consistent with the *in vitro* binding assay data, the P3A p66^{shc} mutant and P3A mutant CH2 domain, which do not bind to Src through the P*XX*P-SH3 interaction, had no effect on Src kinase activity (Fig. 6, *lanes 9* and *10 versus lane 1*; *p*, NS). Similarly, p52^{shc} also had no effect on Src kinase activity (Fig. 6*C*, *lane 11 versus lane 1*; *p*, NS). These data confirm that P*XX*P-SH3 interaction plays a vital role in inhibition of Src activation. However, because full-length p66^{shc} had greater effect than the CH2 domain, this suggests that the SH2-Tyr(P) interaction was also necessary for maximal inhibition.

To determine the importance of the SH2-Tyr(P) interaction, the SH2 domain of p66^{shc} was deleted, and the mutant form was tested for its ability to inhibit Src kinase activity *in vitro*. This p66^{shc} mutant was less effective than full-length p66^{shc} (data not shown). However, when the CH2 domain peptide and p52^{shc}, which binds to Src through SH2-Tyr(P) interaction, were added together, there was no additional effect compared with the CH2 domain alone (Fig. 6*D*, *lane 3 versus lane 5*; *p*, NS).

We used cell-permeable peptides to confirm these results using living cells. IGF-I-stimulated Src activation was impaired following overexpression of WT p66^{shc} (*e.g.* a 2.46 ± 0.15-fold increase in LacZ *versus* a 1.49 ± 0.10-fold increase in p66^{shc} WT after IGF-I stimulation; $p < 0.01$), and this could be reduced by preincubation with p189 (*e.g.* a 1.49 ± 0.10-fold increase in p66^{shc} WT *versus* a 2.57 ± 0.15-fold increase in p66^{shc} WT with p189 preincubation after IGF-I stimulation; $p < 0.01$) (Fig. 7*A*). In addition, we showed that p189 could enhance IGF-I-stimulated Src activation in wild type SMC (data not shown). Although p136 was less effective than p189 in rescuing IGF-I-stimulated Src activation (*e.g.* a 2.70 ± 0.30-fold increase with p136 preincubation *versus* a 3.53 ± 0.46-fold increase in p189 preincubation after IGF-I stimulation; $p < 0.05$, $n = 4$), it had a significant effect (*e.g.* a 2.70 ± 0.30-fold increase in p136 preincubation *versus* a 1.74 ± 0.15-fold increase without preincubation after IGF-I stimulation in p66^{shc} WT cells; $p < 0.05$, $n = 4$) (Fig. 7*B*), suggesting that Tyr(P)-SH2 interaction between Src and p66^{shc} also plays a role in mediating the inhibitory effect of p66^{shc} on Src activation in living cells.

To confirm the results obtained using the peptides, the cells expressing the p66^{shc} P3A and p66^{shc} ΔSH2 mutants were utilized. In cells expressing P3A mutant, IGF-I stimulated Src activation to the same extent as cells expressing LacZ (*e.g.* a 2.00 ± 0.10-fold increase in p66^{shc} P3A cells *versus* a 2.05 ± 0.10-fold increase in LacZ cells after IGF-I stimulation; *p*, NS), whereas cells expressing WT p66^{shc} showed the inhibition of Src activation (*e.g.* a 2.05 ± 0.10-fold increase in LacZ cells *versus* a 1.23 ± 0.09-fold increase in p66^{shc} WT cells after IGF-I stimulation; $p < 0.01$) (Fig. 7*C*). Consistent with peptide data, overexpres-

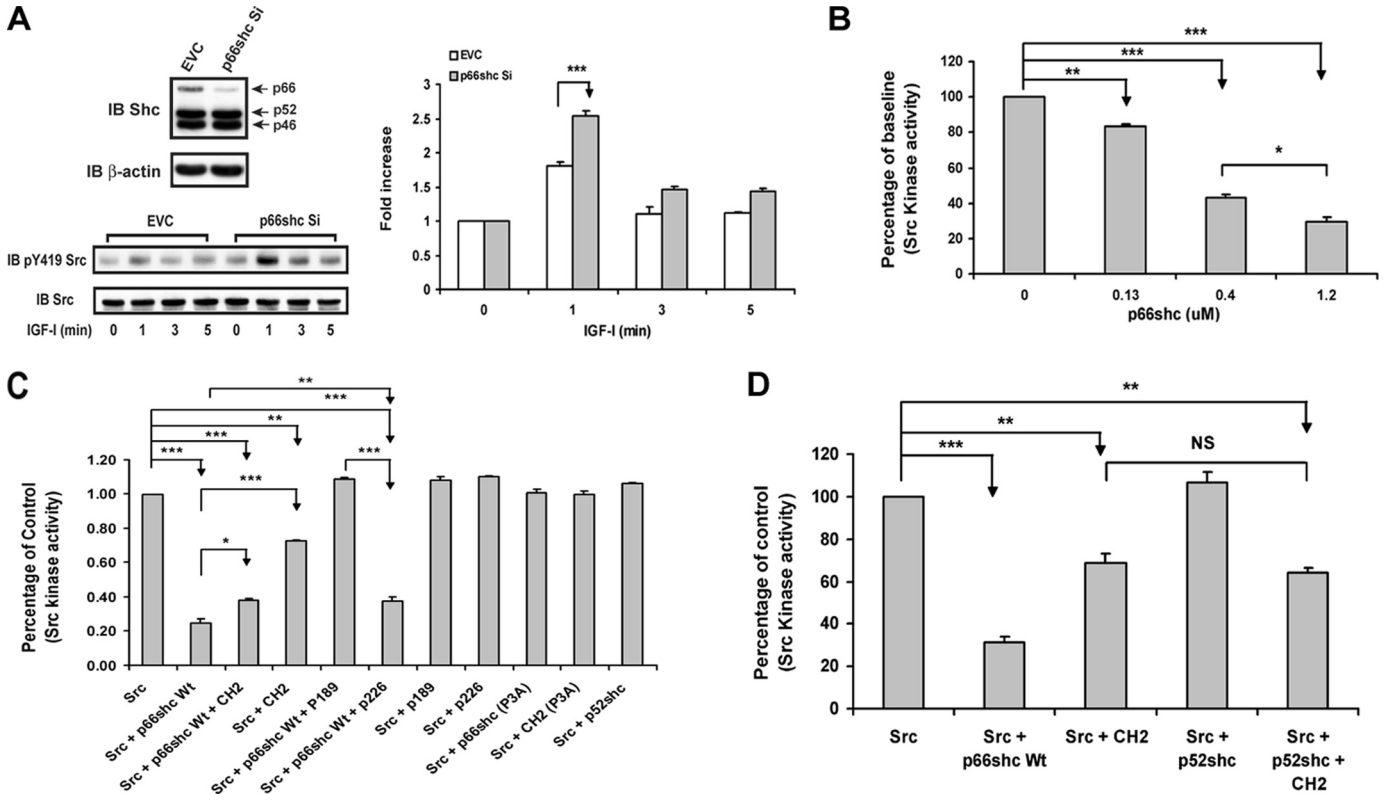

FIGURE 6. **p66^{shc} impairs Src kinase activation through polyproline-SH3 domain interaction *in vitro*.** *A*, after IGF-I treatment (100 ng/ml) for the indicated times, the lysates from empty vector (*EVC*)- and p66^{shc} short hairpin RNA template vector (*p66^{shc} Si*)-transduced cells were used to determine the activation of Src kinase by immunoblotting (*IB*) with an anti-phospho-Tyr^{419} Src antibody. The blot was reprobed with an anti-Src antibody to control for loading differences. $p < 0.001$ (***) indicates that knockdown of p66^{shc} significantly enhances IGF-I-stimulated Src kinase activation, compared with EVC. *B–D*, p66^{shc}, p52^{shc}, p66^{shc} (P3A), CH2, and CH2 (P3A) were expressed using a cell-free system and then incubated with activated Src kinase, and the ability of Src to phosphorylate a peptide substrate *in vitro* was determined as described under "Experimental Procedures." The effect of p189 or p226 was also determined. $p < 0.05$ (*), $p < 0.01$ (**), and $p < 0.001$ (***) indicate the significant differences between the treatment and control or between two different treatments. The figure is representative of three independent experiments.

sion of p66^{shc} ΔSH2 (Fig. 7*D*), which eliminates the Tyr(P)-SH2 interaction between Src and p66^{shc}, still inhibited IGF-I-stimulated Src activation (*e.g.* a 2.68 ± 0.24-fold increase in LacZ cells *versus* a 1.86 ± 0.10-fold increase in p66^{shc} ΔSH2; $p < 0.01$), but it was less effective than full-length p66^{shc} (*e.g.* a 1.86 ± 0.10-fold increase in p66^{shc} ΔSH2 *versus* a 1.32 ± 0.13-fold increase in p66^{shc} WT cells after IGF-I stimulation; $p < 0.05$) (Fig. 7*E*). Based on these data, we conclude that the full inhibitory effect of p66^{shc} on IGF-I-stimulated Src activation requires both P*XX*P-SH3 and Tyr(P)-SH2 interactions but that the inhibitory effect is initiated by the P*XX*P-SH3 interaction.

Examination of the Proposed Mechanism in Porcine Aortic Endothelial Cells—In order to determine whether the proposed mechanism is unique for pSMC or is applicable for all other cell types, we used the porcine aortic endothelial cells to examine several pivotal results. We chose endothelial cells because they express αVβ3, Src, p66^{shc}, and SHPS-1, the major components affecting SHPS-1 complex formation and IGF-I signal transduction, and they have been shown to respond to hyperglycemia by increasing their sensitivity to IGF-I stimulation (28, 29). Similar to pSMC, IGF-I stimulated p66^{shc} association with Src after 1- and 3-min treatment. The interaction at 1 min was disrupted by p189, the polyproline and SH3 domain interaction blocker, but not by tyrosine-phosphorylated p226. Both peptides were able to cause some disruption of the interaction at 3 min after IGF-I stimulation (Fig. 8*A*), which is consistent with the hypothesis that binding occurs through both sites. In addition, IGF-I stimulated Src activation after a 1-min treatment (2.14 ± 0.08-fold increase above the basal level; $p < 0.01$), and this stimulation was enhanced by p189 preincubation (additional 1.53 ± 0.12-fold increase compared with IGF-I alone; $p < 0.01$) but not a control peptide (Fig. 8*B*). To determine the effect on downstream signaling, we examined the p52^{shc} tyrosine phosphorylation and MAPK activation in response to IGF-I. IGF-I stimulated p52^{shc} tyrosine phosphorylation (2.77 ± 0.22-fold increase above basal; $p < 0.01$) and MAPK activation (3.18 ± 0.18-fold increase above basal; $p < 0.01$). Importantly, these responses were enhanced by p189 but not a control peptide (Fig. 8, *C* and *D*). To determine the effect of disruption of Src-p66^{shc}, on IGF-I-stimulated biological actions, we examined IGF-I-stimulated cell proliferation in the presence of p189 or a control peptide. IGF-I-stimulated cell proliferation was enhanced by p189 preincubation (1.87 ± 0.09-fold *versus* 2.38 ± 0.08-fold increase after IGF-I treatment; $p < 0.05$), but exposure to the control peptide had no effect (1.87 ± 0.09-fold *versus* 1.76 ± 0.07-fold increase after IGF-I treatment; *p*, NS) (Fig. 8*E*).

DISCUSSION

Our prior studies have shown that in response to hyperglycemia, a signaling complex composed of the scaffolding protein

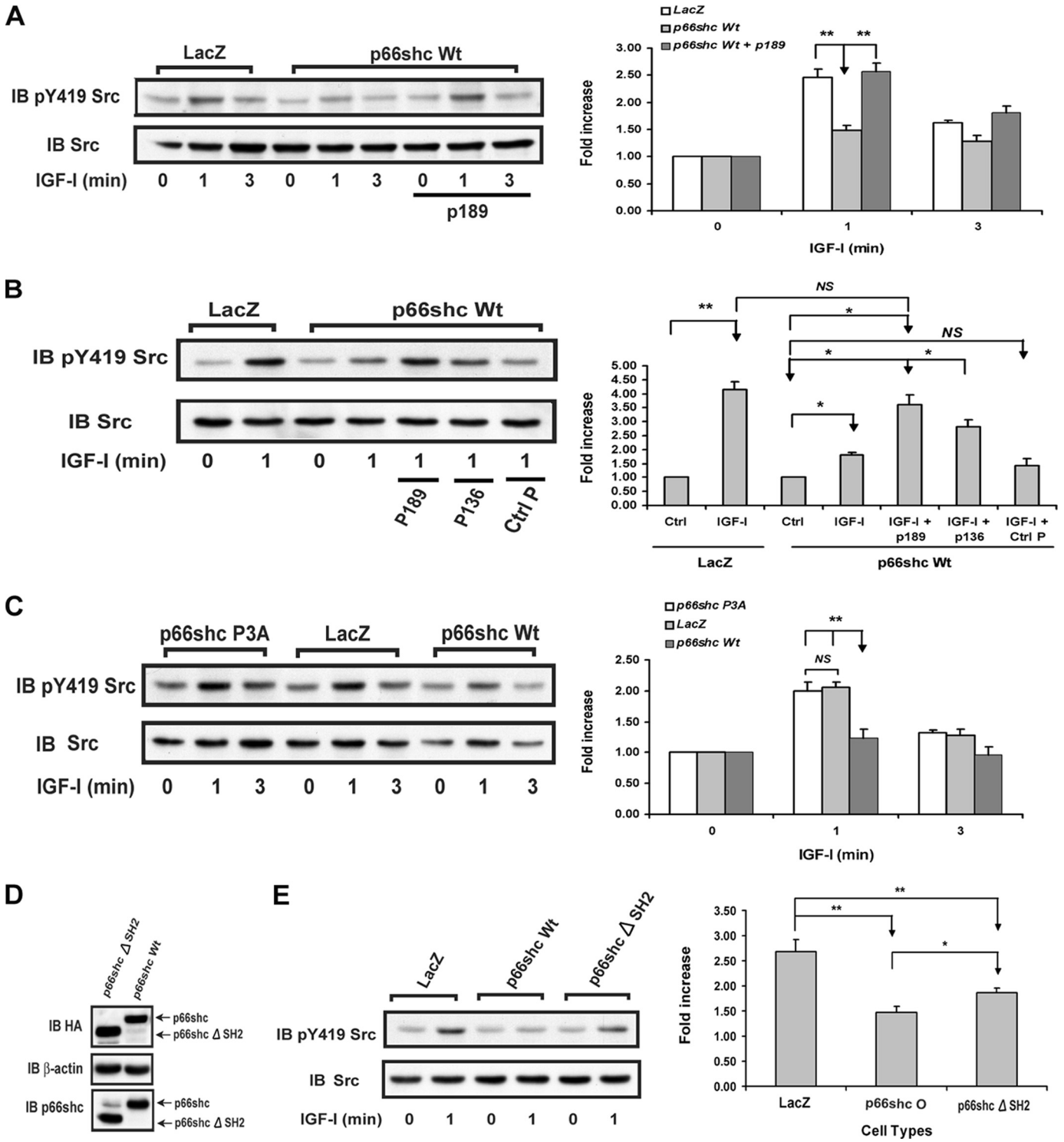

FIGURE 7. **p66^{shc} impairs IGF-I-stimulated Src kinase activation through polyproline-SH3 domain and SH2-phosphotyrosine interactions in living cells.** *A–C*, quiescent LacZ, WT p66^{shc} (*p66^{shc} WT*)-, and p66^{shc} P3A-overexpressing cells were preincubated with or without p189 or p136 for 2 h before stimulation with IGF-I (100 ng/ml) for the indicated times. The activation of Src kinase was measured by probing with an anti-phospho-Tyr^{419} Src antibody. The blots were reprobed with an anti-Src antibody to control for loading differences. $p < 0.05$ (*) and $p < 0.01$ (**) indicate the significant differences between two different treatments or the same treatment in two cell types. *D*, pSMC were transduced with pLenti-p66^{shc} WT-HA (p66^{shc} WT) or pLenti-p66^{shc} ΔSH2-HA (*p66^{shc} ΔSH2*) vector. Both cell types were serum-starved for 16–18 h and analyzed for HA and p66^{shc} protein expression. Cell lysates were immunoblotted with anti-HA and p66^{shc} antibodies. The *arrows* denote the 66-kDa and SH2-deleted p66^{shc} forms. *E*, quiescent LacZ, p66^{shc} WT, and p66^{shc} ΔSH2 cells were stimulated with IGF-I (100 ng/ml) for the indicated times. Cell lysates were immunoblotted with an anti-phospho-Tyr^{419} Src antibody. To control for loading, the blot was reprobed with an anti-Src antibody. $p < 0.01$ (**) and $p < 0.05$ (*) indicate the significant differences between two cell types. The figure is representative of at least three independent experiments. *IB*, immunoblot; *Ctrl*, control.

SHPS-1, SHP-2, Src, and p52^{shc} is formed following IGF-I stimulation. This complex is essential for IGF-I-stimulated p52^{shc} and MAPK activation and cell proliferation in vascular cell types (7). p52^{shc} is recruited to this complex by Src, which then phosphorylates three tyrosines (24), leading to Grb2 recruitment and MAPK activation. In contrast to p52^{shc}, the p66^{shc}

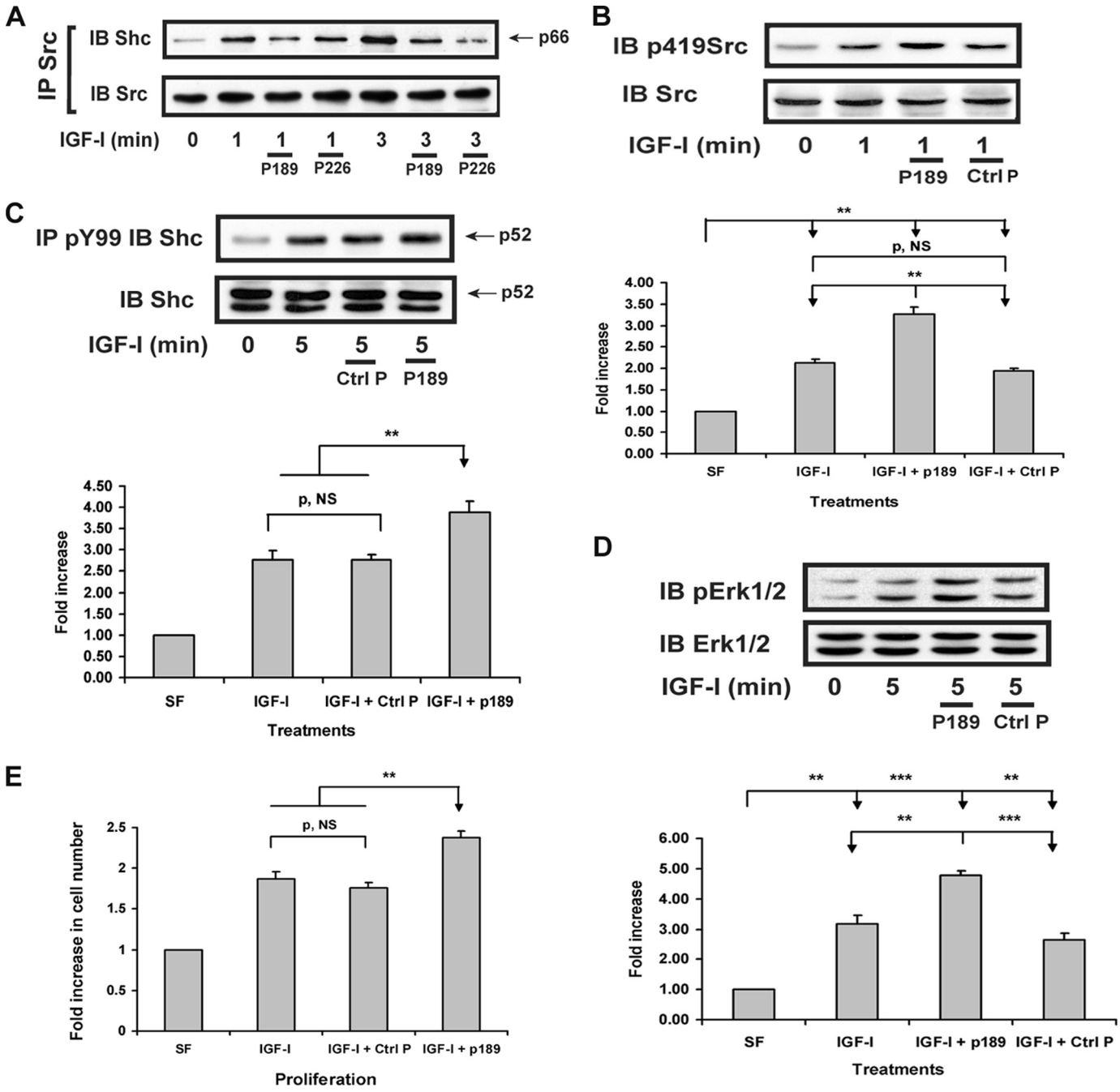

FIGURE 8. **The proposed mechanism is also utilized in porcine aortic endothelial cells.** *A*, endothelial cells were serum-starved for 16–18 h and preincubated with p189 or p226 (5 μM) for 2 h before adding IGF-I (100 ng/ml) for the indicated times. The cell lysates were immunoprecipitated (*IP*) with an anti-Src antibody and immunoblotted (*IB*) with an anti-Shc antibody. To control the loading, the blot was reprobed with an anti-Src antibody. The *arrow* denotes the p66^{shc} band. *B*, quiescent endothelial cells were preincubated with p189 or a control peptide (5 μM) for 2 h before adding IGF-I (100 ng/ml) for 1 min. The activation of Src kinase was measured by probing with an anti-phospho-Tyr^{419} Src antibody. The blots were reprobed with an anti-Src antibody to control for loading differences. *C*, quiescent endothelial cells were preincubated with p189 or a control peptide (5 μM) for 2 h before adding IGF-I (100 ng/ml) for 5 min. The cell lysates were immunoprecipitated with an anti-Tyr(P) (*pY99*) antibody and immunoblotted with an anti-Shc antibody. To control the loading, an equal amount of cell lysate was immunoblotted with an anti-Shc antibody. The *arrow* denotes the p52^{shc} band. *D*, the same cell lysates were used to determine the Erk1/2 phosphorylation by probing with an anti-phospho-Erk1/2 antibody. The blots were reprobed with an anti-Erk1/2 antibody to control for loading differences. *E*, cell proliferation was determined as described under "Experimental Procedures". Each *bar* indicates the fold increase over basal and represents the pool of at least three independent experiments. $p < 0.01$ (**) and $p < 0.001$ (***) indicate the significant differences between two different treatments. The figure is representative of three independent experiments.

isoform, which is also increased in response to hyperglycemia, inhibits IGF-I-stimulated SHPS-1 complex formation and p52^{shc} recruitment to this complex, resulting in impaired Grb2 binding and MAPK activation, cell proliferation, and migration in response to IGF-I (10). In the present study, we have determined the mechanism by which p66^{shc} disrupts IGF-I-stimulated p52^{shc} recruitment and activation. The results demonstrate that p66^{shc} sequentially binds to Src via a P*XX*P-SH3 interaction, followed by a SH2-Tyr(P) interaction, in response to IGF-I, and this leads to impairment of IGF-I-stimulated Src

kinase activation, resulting in attenuated IGF-I-stimulated p52^{shc} phosphorylation and impaired MAPK activation, SMC proliferation, and migration.

To understand how p66^{shc} inhibits IGF-I-stimulated p52^{shc}-dependent signaling, several potential mechanisms were analyzed. Previous studies had proposed that EGF-dependent association of Grb2 with p66^{shc} interfered with the ability of Grb2 to recruit SOS (son of sevenless), leading to attenuated activation of MAPK (2), or that overexpression of p66^{shc} competed with p52^{shc} for binding to a limited pool of Grb2, resulting in impaired p52^{shc} association and MAPK activation (9). In contrast, our results showed that p66^{shc} 3F mutant, which does not bind to Grb2, still inhibited the recruitment of Grb2 to p52^{shc} to the same extent as wild type p66^{shc} (Fig. 1*C*). Therefore, we focused on the role of the unique CH2 domain of p66^{shc} in attenuating p52^{shc} phosphorylation. Because a polyproline sequence was identified in the p66^{shc} CH2 domain and a SH3 domain is contained in Src, we investigated whether this interaction was modulating Src kinase activation. Our *in vitro* binding assay results showed that p66^{shc} bound directly to the SH3 domain of Src through a PILPPLP sequence contained in the CH2 domain. Further analyses using intact SMC indicated that p66^{shc} bound to Src not only via the P*XX*P-SH3 interaction but also through a SH2 domain and Tyr(P) interaction in response to IGF-I. Using specific blocking peptides and SMC expressing a variety of mutants, we were able to show that these binding interactions occurred sequentially after IGF-I stimulation, the P*XX*P-SH3 interaction (detected at the 1 min time point) occurring earlier than the SH2-Tyr(P) interaction (detected at the 3 min time point). Importantly, similar results were obtained in non-p66^{shc}-overexpressing cells (LacZ cells) and non-transduced wild type pSMC (Fig. 3, *B* and *C*).

Because extensive studies have shown that Src activation depends on its conformational structure (30, 31), we investigated if p66^{shc} binding to Src would alter IGF-I-stimulated Src kinase activation. The Src kinase domain is maintained in an inactive state by intramolecular interactions (32, 33). Several mechanisms have been proposed for activation of Src kinase, including replacement of either SH2- or SH3-mediated intramolecular interactions by high affinity ligands, such as autophosphorylated platelet-derived growth factor receptor (34), a P*XX*P motif-containing protein (35); inactivation of Csk (C-terminal Src tyrosine kinase) and Chk (Csk homologous kinase); and dephosphorylation of tyrosine 530 (equivalent to Tyr^{527} in chick Src) by tyrosine phosphatases (36, 37). Herein, we report a novel mechanism for regulating IGF-I-dependent Src kinase activation. Our findings show that the CH2 domain of p66^{shc} contains a P*XX*P motif that binds directly to the SH3 domain in Src, and this complex formation initiates a series of events leading to the inhibition of Src activation. To our best knowledge, this study is the first to show that a Src-SH3 domain-P*XX*P ligand interaction can inhibit Src kinase activation in response to stimuli. In contrast, the P*XX*P-SH3 interaction has been shown to induce Src family kinase activation (35, 38, 39). Although "turn on by a touch" is a widely accepted mechanism for activation of Src and other members of the Src family kinases, the actual steps leading to kinase activation are more complex, and kinase activation depends on the spatial positions and conformations of the SH3 and SH2 domains, the kinase loop, the activation loop, and the C helix (40). Theoretically, an alteration in any of these steps could prevent the kinase activation. Therefore, it is possible that the SH3 domain binding interaction induces an allosteric change and thereby inhibits Src kinase activation. In support of our observations, prior studies have shown that proteins binding to Src family kinases through non-SH3 domain interactions can inhibit kinase activation. These include the non-catalytic domain of Chk (41), RACK1 (receptor of activated protein C kinase) (42), caveolin (43), and Wiskott-Aldrich syndrome protein (44).

To understand the underlying mechanism of the inhibitory effect of p66^{shc}, several different approaches were employed. *In vitro* kinase assays showed that full-length WT p66^{shc} directly inhibited Src kinase activity, and this inhibitory effect could be reversed by the P*XX*P-SH3 blocking peptide. In addition, the CH2 domain of p66^{shc} had an inhibitory effect on Src kinase activity, whereas p66^{shc} P3A mutant and P3A-mutated CH2 domain had no effect on Src activation (Fig. 6). The studies using living cells showed that IGF-I-stimulated Src activation was significantly attenuated by overexpression of WT p66^{shc}, and this effect could be nullified by the addition of a peptide containing the P*XX*P motif or enhanced by knockdown of p66^{shc}. Additionally, the expression of p66^{shc} P3A mutant had no effect on IGF-I-stimulated Src kinase activation in living cells. These results clearly indicate that P*XX*P sequences in the CH2 domain of p66^{shc} interact with the SH3 domain in Src, resulting in inhibition of Src kinase activation. Although the P*XX*P region mediates the inhibition, it is insufficient to inhibit Src kinase activation, which requires the full-length CH2 domain. Of note, full-length p66^{shc} had an even greater effect than the CH2 domain, suggesting that the SH2 domain interaction with Tyr(P)^{329} or Tyr(P)^{360} in Src is required for maximal inhibition of Src activation. This prediction is supported by the observation that the Tyr(P)-SH2 blocking peptide partially attenuated the inhibitory effect of p66^{shc} on Src kinase activity in the *in vitro* kinase assay (Fig. 6*C*) and that it could partially rescue IGF-I-stimulated Src activation in WT p66^{shc}-overexpressing cells, although it was less effective than the P*XX*P-SH3 blocking peptide (Fig. 7*B*). However, once P*XX*P-SH3 interaction was disrupted, the Tyr(P)-SH2 interaction no longer had an effect on IGF-I-stimulated Src activation. This is consistent with our results showing that expression of the full-length p66^{shc} P3A mutant was unable to inhibit IGF-I-stimulated Src kinase activation. Therefore, we believe that SH3-P*XX*P interaction serves to initiate the inhibitory effect of p66^{shc} on Src activation in response to IGF-I and that the Tyr(P)-SH2 interaction also contributes to the inhibitory effect. Formation of P*XX*P-SH3 interaction alone allowed some (but not complete) inhibition by p66^{shc}, even though the SH2-Tyr(P) interaction could not be established (*e.g.* p66^{shc} SH2 domain deletion) (Fig. 7, *D* and *E*). Our data indicate that simply occupying either of the binding sites or both sites did not confer the full inhibitory effect, since neither peptide itself could inhibit Src kinase activity (Fig. 6*C*), and the addition of the CH2 domain peptide plus p52^{shc} did not have an additional inhibitory effect compared with CH2 peptide alone (Fig. 6*D*). Based on these results, we postulate that IGF-I treatment triggers the conformation

change of inactive (folded) Src and slightly opens its folded structure. This allows the p66^{shc} to bind to it via a P*XX*P-SH3 interaction. Meanwhile, after IGF-I treatment, Src autophosphorylates Tyr^{329} and Tyr^{360}, which allows the further binding to p66^{shc} via a SH2-Tyr(P) interaction. When binding is present at both sites, p66^{shc} can significantly inhibit Src activation either by preventing further Src unfolding or by inducing an allosteric change to inactivate kinase activity. Our *in vitro* Src kinase assay data clearly showed that at least the latter mechanism was present because when p66^{shc} was added into the activated Src, the kinase activity of Src was significantly reduced (Fig. 6*C*). To support this proposed model, RACK1 has been reported to inhibit Src kinase activation via interaction through multiple binding sites, including SH2 domain of Src, and acts as a molecular chaperone to hold Src in the closed and inactive conformational state (42). Similarly, Hsp90, a chaperone protein, has also been shown to hold v-Src in the inactive state, thereby inhibiting its activation (45). In addition, this model allows us to explain an interesting observation that shows that, in LacZ cells, IGF-I stimulated p66^{shc}·Src complex formation after 1 min of treatment, and the complex formation continued increasing after 3 min of IGF-I treatment, whereas, in p66^{shc}-overexpressing cells, the maximal complex formation was detected after 1 min of IGF-I treatment, and no further increase was detected at the 3 min time point (Fig. 3*A*). We believe that is because, in p66^{shc}-overexpressing cells, the formation a large amount of the p66^{shc}·Src complex via the P*XX*P-SH3 interaction at 1 min inhibits Src autophosphorylation. Because Src activation has been shown to be essential for phosphorylation of Src Tyr^{329} and Tyr^{360} (24), which provide the binding sites for SH2 domain in p66^{shc}, this inhibition of Src kinase activity limits the further increase of the complex formation via the SH2-Tyr(P) interaction. By contrast, in LacZ cells, the degree of increase in p66^{shc} binding to Src via a P*XX*P-SH3 interaction at 1 min does not significantly inhibit Src activation in response to IGF-I, and this permits the formation of additional p66^{shc}·Src complex via the SH2-Tyr(P) interaction at the 3 min time point. Because the SH2-Tyr(P) interaction has a higher affinity than P*XX*P-SH3 domain interaction, it is reasonable to expect the greater p66^{shc}·Src complex formation via the SH2-Tyr(P) interaction at this time point. Consequently, it is not surprising that p136 or p226, both of which inhibit the SH2-Tyr(P) interaction, has a greater inhibitory effect than p189 on the formation of p66^{shc}·Src complex after 3 min of IGF-I treatment (Fig. 3, *B* and *C*).

Previous studies have shown that IGF-I activates Src kinase, and this activation is critical for mediating IGF-I downstream signaling, such as MAPK activation (24, 46, 47), Akt activation (48), and IGF-I-stimulated biological actions (24, 49). To understand the mechanism of Src-mediated IGF-I signaling, previous studies focused on the identification of Src kinase substrate, revealing that p52^{shc} was a good candidate. Both *in vitro* and *in vivo* data showed that activated Src can phosphorylate p52^{shc} on Tyr^{239}/Tyr^{240}/Tyr^{317} (50, 51). Our previous study clearly demonstrated that, upon IGF-I stimulation, Src recruited p52^{shc} to the SHPS-1 signaling complex and phosphorylated Tyr^{239}/Tyr^{240}/Tyr^{317} on p52^{shc}, providing a binding site for Grb2, thus activating downstream signaling in SMC (24). This SHPS-1 complex formation is essential for IGF-I-stimulated MAPK activation and biological actions (7). Disruption of this complex formation by truncation of the SHPS-1 cytoplasmic domain (7) or Src silencing (24) or by overexpression of p66^{shc} (10) leads to impaired IGF-I signaling and biological actions. Our previous and current data have shown that IGF-I-induced Src activation is quite rapid and transient; the highest level is detected at 1 min and then reduced after 3 or 5 min in pSMC (24) (Figs. 6–8). Consistent with our findings, a similar pattern in IGF-I-stimulated Src activation was observed in preadipocytes (46). Consequently, an obvious question is how this rapid and transient activated Src phosphorylates p52^{shc} on the SHPS-1 signaling complex and mediates MAPK activation at the late time points. To address this question, we investigated the kinetic activation of Src in response to IGF-I stimulation, showing that the activation of Src occurred at 1 min but was still greater than the basal activation level at 10 and 30 min after IGF-I stimulation (supplemental Fig. 1*A*). More importantly, we used co-immunoprecipitation to show that SHPS-1-associated p419Src (which phosphorylates p52^{shc}) increased progressively after 5 and 10 min of IGF-I stimulation (supplemental Fig. 1*B*). These findings support our previous data indicating that Src is recruited to the SHPS-1 complex and remains active at a time when p52^{shc} is phosphorylated, leading to Erk1/2 activation in response to IGF-I treatment. Because activation of IGF-I signaling has been shown to inhibit hyperglycemia-induced DNA damage (52) and activation of the mitochondrial apoptosis program (53), it is possible that a major increase in p66^{shc} may impair the ability of IGF-I to rescue cells under these conditions. This is consistent with the observation that p66^{shc} can induce apoptosis under conditions of increased oxidative stress or hyperglycemia (54). However, our findings suggest that these responses are dependent upon the level of p66^{shc} and Src activation.

To expand the applicability of our findings, we examined the proposed mechanism in the endothelial cells and confirmed the pivotal molecular events that we observed in pSMC. Endothelial cells express $\alpha v\beta 3$, Src, p66^{shc}, and SHPS-1, which are required for studying SHPS-1 signaling complex formation and modulation of IGF-I signal transduction in hyperglycemia. In addition, they have been shown to respond to hyperglycemia by increasing their sensitivity to IGF-I stimulation (28, 29). Therefore, we believe that this mechanism at least is applicable to specific cell types that have the capability to respond to hyperglycemic and/or oxidative stress with an increase in proliferation in response to IGF-I.

In summary, our data demonstrate that p66^{shc} sequentially binds to Src through a P*XX*P-SH3 and a SH2-Tyr(P) interaction in response to IGF-I. The P*XX*P-SH3 interaction plays a major role in initiating the inhibition of IGF-I-stimulated Src kinase activation; however, the full inhibitory effect requires the presence of the SH2-Tyr(P) interaction. This inhibition leads to impairment of IGF-I-dependent p52^{shc} tyrosine phosphorylation, MAPK activation, and IGF-I-stimulated cell proliferation and migration. Our findings provide novel information regarding the regulation of Src kinase activation and suggest new possible strategies for inhibiting constitutively activated Src kinase and p52^{shc} signaling.

Acknowledgments—We thank Dr. Laura Maile for providing porcine aortic endothelial cells, Dr. Jane Badley-Clarke for help in p66shc 3F construction, and Laura Lindsey for help in preparing the manuscript.

REFERENCES

1. Pelicci, G., Lanfrancone, L., Grignani, F., McGlade, J., Cavallo, F., Forni, G., Nicoletti, I., Grignani, F., Pawson, T., and Pelicci, P. G. (1992) *Cell* **70,** 93–104
2. Migliaccio, E., Mele, S., Salcini, A. E., Pelicci, G., Lai, K. M., Superti-Furga, G., Pawson, T., Di Fiore, P. P., Lanfrancone, L., and Pelicci, P. G. (1997) *EMBO J.* **16,** 706–716
3. Ravichandran, K. S. (2001) *Oncogene* **20,** 6322–6330
4. Sasaoka, T., Ishiki, M., Wada, T., Hori, H., Hirai, H., Haruta, T., Ishihara, H., and Kobayashi, M. (2001) *Endocrinology* **142,** 5226–5235
5. Boney, C. M., Gruppuso, P. A., Faris, R. A., and Frackelton, A. R., Jr. (2000) *Mol. Endocrinol.* **14,** 805–813
6. Ursini-Siegel, J., Hardy, W. R., Zuo, D., Lam, S. H., Sanguin-Gendreau, V., Cardiff, R. D., Pawson, T., and Muller, W. J. (2008) *EMBO J.* **27,** 910–920
7. Ling, Y., Maile, L. A., Lieskovska, J., Badley-Clarke, J., and Clemmons, D. R. (2005) *Mol. Biol. Cell* **16,** 3353–3364
8. Maile, L. A., Capps, B. E., Miller, E. C., Aday, A. W., and Clemmons, D. R. (2008) *Diabetes* **57,** 2637–2643
9. Okada, S., Kao, A. W., Ceresa, B. P., Blaikie, P., Margolis, B., and Pessin, J. E. (1997) *J. Biol. Chem.* **272,** 28042–28049
10. Xi, G., Shen, X., and Clemmons, D. R. (2008) *Mol. Endocrinol.* **22,** 2162–2175
11. Migliaccio, E., Giorgio, M., Mele, S., Pelicci, G., Reboldi, P., Pandolfi, P. P., Lanfrancone, L., and Pelicci, P. G. (1999) *Nature* **402,** 309–313
12. Favetta, L. A., Robert, C., King, W. A., and Betts, D. H. (2004) *Exp. Cell Res.* **299,** 36–48
13. Favetta, L. A., Madan, P., Mastromonaco, G. F., St John, E. J., King, W. A., and Betts, D. H. (2007) *BMC Dev. Biol.* **7,** 132
14. Orsini, F., Migliaccio, E., Moroni, M., Contursi, C., Raker, V. A., Piccini, D., Martin-Padura, I., Pelliccia, G., Trinei, M., Bono, M., Puri, C., Tacchetti, C., Ferrini, M., Mannucci, R., Nicoletti, I., Lanfrancone, L., Giorgio, M., and Pelicci, P. G. (2004) *J. Biol. Chem.* **279,** 25689–25695
15. Camici, G. G., Schiavoni, M., Francia, P., Bachschmid, M., Martin-Padura, I., Hersberger, M., Tanner, F. C., Pelicci, P., Volpe, M., Anversa, P., Lüscher, T. F., and Cosentino, F. (2007) *Proc. Natl. Acad. Sci. U.S.A.* **104,** 5217–5222
16. Chintapalli, J., Yang, S., Opawumi, D., Goyal, S. R., Shamsuddin, N., Malhotra, A., Reiss, K., and Meggs, L. G. (2007) *Am. J. Physiol. Renal Physiol.* **292,** F523–F530
17. Trinei, M., Giorgio, M., Cicalese, A., Barozzi, S., Ventura, A., Migliaccio, E., Milia, E., Padura, I. M., Raker, V. A., Maccarana, M., Petronilli, V., Minucci, S., Bernardi, P., Lanfrancone, L., and Pelicci, P. G. (2002) *Oncogene* **21,** 3872–3878
18. Menini, S., Amadio, L., Oddi, G., Ricci, C., Pesce, C., Pugliese, F., Giorgio, M., Migliaccio, E., Pelicci, P., Iacobini, C., and Pugliese, G. (2006) *Diabetes* **55,** 1642–1650
19. Chen, Y., Capron, L., Magnusson, J. O., Wallby, L. A., and Arnqvist, H. J. (1998) *Growth Horm. IGF Res.* **8,** 299–303
20. Campbell, M., Allen, W. E., Silversides, J. A., and Trimble, E. R. (2003) *Diabetes* **52,** 519–526
21. Campbell, M., and Trimble, E. R. (2005) *Circ. Res.* **96,** 197–206
22. Ruiz, E., Gordillo-Moscoso, A., Padilla, E., Redondo, S., Rodriguez, E., Reguillo, F., Briones, A. M., van Breemen, C., Okon, E., and Tejerina, T. (2006) *Diabetes* **55,** 1243–1251
23. Maile, L. A., Capps, B. E., Ling, Y., Xi, G., and Clemmons, D. R. (2007) *Endocrinology* **148,** 2435–2443
24. Lieskovska, J., Ling, Y., Badley-Clarke, J., and Clemmons, D. R. (2006) *J. Biol. Chem.* **281,** 25041–25053
25. Gockerman, A., and Clemmons, D. R. (1995) *Circ. Res.* **76,** 514–521
26. Nam, T. J., Busby, W. H., Jr., Rees, C., and Clemmons, D. R. (2000) *Endocrinology* **141,** 1100–1106
27. Jones, J. I., Prevette, T., Gockerman, A., and Clemmons, D. R. (1996) *Proc. Natl. Acad. Sci. U.S.A.* **93,** 2482–2487
28. Shigematsu, S., Yamauchi, K., Nakajima, K., Iijima, S., Aizawa, T., and Hashizume, K. (1999) *Endocr. J.* **46,** (suppl.) S59–S62
29. Miller, E. C., Capps, B. E., Sanghani, R. R., Clemmons, D. R., and Maile, L. A. (2007) *Invest. Ophthalmol. Vis. Sci.* **48,** 3878–3887
30. Yang, S., and Roux, B. (2008) *PLoS Comput. Biol.* **4,** e1000047
31. Cowan-Jacob, S. W., Fendrich, G., Manley, P. W., Jahnke, W., Fabbro, D., Liebetanz, J., and Meyer, T. (2005) *Structure* **13,** 861–871
32. Murphy, S. M., Bergman, M., and Morgan, D. O. (1993) *Mol. Cell Biol.* **13,** 5290–5300
33. Xu, W., Doshi, A., Lei, M., Eck, M. J., and Harrison, S. C. (1999) *Mol. Cell* **3,** 629–638
34. Alonso, G., Koegl, M., Mazurenko, N., and Courtneidge, S. A. (1995) *J. Biol. Chem.* **270,** 9840–9848
35. Saksela, K., Cheng, G., and Baltimore, D. (1995) *EMBO J.* **14,** 484–491
36. Abram, C. L., and Courtneidge, S. A. (2000) *Exp. Cell Res.* **254,** 1–13
37. Alper, O., and Bowden, E. T. (2005) *Curr. Pharm. Des.* **11,** 1119–1130
38. Moarefi, I., LaFevre-Bernt, M., Sicheri, F., Huse, M., Lee, C. H., Kuriyan, J., and Miller, W. T. (1997) *Nature* **385,** 650–653
39. Chan, B., Lanyi, A., Song, H. K., Griesbach, J., Simarro-Grande, M., Poy, F., Howie, D., Sumegi, J., Terhorst, C., and Eck, M. J. (2003) *Nat. Cell Biol.* **5,** 155–160
40. Boggon, T. J., and Eck, M. J. (2004) *Oncogene* **23,** 7918–7927
41. Chong, Y. P., Mulhern, T. D., Zhu, H. J., Fujita, D. J., Bjorge, J. D., Tantiongco, J. P., Sotirellis, N., Lio, D. S., Scholz, G., and Cheng, H. C. (2004) *J. Biol. Chem.* **279,** 20752–20766
42. Chang, B. Y., Conroy, K. B., Machleder, E. M., and Cartwright, C. A. (1998) *Mol. Cell Biol.* **18,** 3245–3256
43. Li, S., Couet, J., and Lisanti, M. P. (1996) *J. Biol. Chem.* **271,** 29182–29190
44. Schulte, R. J., and Sefton, B. M. (2003) *Biochemistry* **42,** 9424–9430
45. Brugge, J. S. (1986) *Curr. Top. Microbiol. Immunol.* **123,** 1–22
46. Boney, C. M., Sekimoto, H., Gruppuso, P. A., and Frackelton, A. R., Jr. (2001) *Cell Growth Differ.* **12,** 379–386
47. Sekimoto, H., Eipper-Mains, J., Pond-Tor, S., and Boney, C. M. (2005) *Mol. Endocrinol.* **19,** 1859–1867
48. Cui, Q. L., Zheng, W. H., Quirion, R., and Almazan, G. (2005) *J. Biol. Chem.* **280,** 8918–8928
49. Knowlden, J. M., Hutcheson, I. R., Barrow, D., Gee, J. M., and Nicholson, R. I. (2005) *Endocrinology* **146,** 4609–4618
50. van der Geer, P., Wiley, S., Gish, G. D., and Pawson, T. (1996) *Curr. Biol.* **6,** 1435–1444
51. Sato, K., Gotoh, N., Otsuki, T., Kakumoto, M., Aoto, M., Tokmakov, A. A., Shibuya, M., and Fukami, Y. (1997) *Biochem. Biophys. Res. Commun.* **240,** 399–404
52. Yang, S., Chintapalli, J., Sodagum, L., Baskin, S., Malhotra, A., Reiss, K., and Meggs, L. G. (2005) *Am. J. Physiol. Renal Physiol.* **289,** F1144–1152
53. Kang, B. P., Frencher, S., Reddy, V., Kessler, A., Malhotra, A., and Meggs, L. G. (2003) *Am. J. Physiol. Renal Physiol.* **284,** F455–F466
54. Pellegrini, M., Pacini, S., and Baldari, C. T. (2005) *Apoptosis* **10,** 13–18